

# **Final Report for Contract No. 3000722487 on Sediment Stability of Bellevue Marine Park (BMP) and Area East of BMP (EBMP) in St. Mary's River, Ontario.**

## **Preamble:**

In this report, the sediment stability at Bellevue Marine Park (BMP) and area east of BMP (EBMP) in St. Mary's River near Sault Ste Marie was analysed using a modelling strategy developed by Krishnappan (2011). The original modelling work carried by Krishnappan (2011) used a coarse time scale of monthly average flows to analyse the stability of the sediment deposits in this area. In the current study, daily average flow rates measured during the time period from April 2002 to present were used together with a maximum flow rate that can be physically released from the lake were used to reassess the stability of the deeper contaminated sediment in BMP and EBMP areas. The numerical grid of the original model was also modified to refine the flow predictions in this area. The revised model was tested against original model to ascertain that the revised model was formulated correctly. A flow duration analysis of the flow data revealed that the flow regime in the river has shifted to a higher regime since 2014 and a 50% exceedance value for the new regime, which was calculated to be 2440 m<sup>3</sup>/s was selected as one of the flows that will be tested with the refined grid model. The other flow rates that were selected for the model simulations were 3657 m<sup>3</sup>/s, which was highest recorded daily average flow rate measured on the 6<sup>th</sup> of August 2005, and 4300 m<sup>3</sup>/s, which was considered to be maximum flow that that can be physically released from the lake.

Model simulations were performed for these three flow rates and the flow properties including the bed shear stresses were calculated. Using the bed shear stress values and the sediment bed stability criterion developed by Krishnappan (2011), the stability of the sediment deposits in BMP and EBMP were reassessed. The reassessment confirmed that the extent of the stable sediment deposit area was a function of the flow rate and the area decreased as the flow rate increased. However, the decreament of the area showed a levelling off tendency, which suggests that a certain portion of the sediment deposits in this area are likely to be present for a foreseeable future.

**Bommanna Krishnappan**

# **Final Report for Contract No. 3000722487 on Sediment Stability of Bellevue Marine Park (BMP) and Area East of BMP (EBMP) in St. Mary's River, Ontario.**

By

**Bommanna G. Krishnappan.**

## **Introduction:**

St. Mary's River has been identified as an area of concern (AOC) under the Canada- US Great Lakes Water Quality agreement (GLWQA) and it requires remedial action plans to address the sediment quality issues in the depositional zones in the river. Embayment areas in the immediate vicinity of the Bellevue Marine Park (BMP) and the area east of the Bellevue Marine Park (EBMP) are identified as areas requiring remedial action. Embayment areas are prone to sediment deposition and exhibit sediment quality issues due to the legacy sediments that were contaminated due to developments in the lower parts of Lake Superior near the entrance of the river. The stability of these sediment deposits needs to be understood in order to address the deleterious effect of contaminated sediment deposits.

Krishnappan (2011) formulated a modelling strategy to predict the flow field and the transport of sediment in the St. Mary's River. Using this modelling strategy, Krishnappan (2011) examined the stability of the sediment deposits in BMP and EBMP using monthly average flows during the period of 1900 to 2009. He demonstrated that the sediment deposits in these areas are stable below a fluff layer of 5 cm.

Recently, it was felt that the monthly average flows used in the model may be too for "coarse" for the analysis of sediment stability: A short term average such as a daily average flows may be more appropriate. Moreover, the impact of climate change which is likely to result in higher than the observed historical flows needs to be taken into account. As a result, the present contract was issued to Dr. Krishnappan to rerun the model using daily average flows over the period when such measurements are available and an additional hypothetical high flow of 4300 m<sup>3</sup>/s (maximum flow that can be physically released from the lake). In addition, it was suggested that a refinement of the numerical grid corresponding to the areas of BMP and EBMP be carried out to enhance the definition of possible eddies and the prediction of flow velocities and bed shear stresses in these areas.

In this final report, the work carried out as part of this contract is described. The work under this contract involved the refinement of the original numerical grid for the areas of BMP and EBMP, updating the original model using the refined grid, the comparison of model results from the original grid model and the refined grid model to demonstrate that the refined grid model has been implemented correctly, testing of different flow scenarios using the refined grid

model and finally, a reassessment of sediment stability at BMP and EBMP areas to confirm if deeper contaminated sediments in these areas are stable under various flow conditions.

### **Refinement of Numerical grid for BMP and EBMP:**

The original grid used in the model of Krishnappan (2011) for the area in the vicinity of BMP and EBMP is shown in Fig. 1 and the refined grid for the same area is shown in Fig.2.

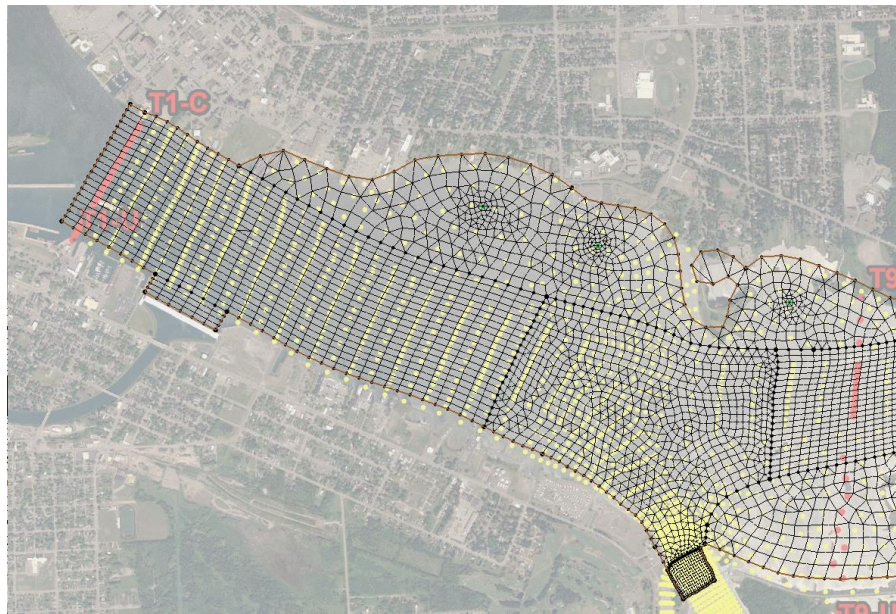


Fig. 1. Original grid of the numerical model of Krishnappan (2011) for the area of BMP and EBMP.

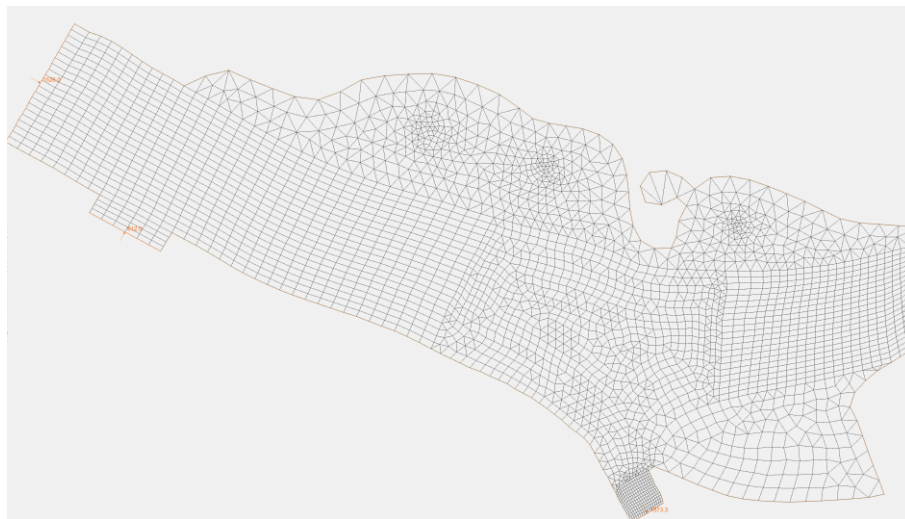


Fig. 2. Refined grid for the BMP and EBMP areas.

The refinement of the grid was implemented by converting the quadrilateral elements in the original grid in the BMP and EBMP area to triangular elements, which increased the number of computational nodes in the finite element mesh of the model. The characteristics of the grid before and after refinement are summarized in Table 1.

Table1. Characteristics of the original and refined grids for the numerical model of the St. Mary's River.

<b>Grid characteristics</b>	<b>Original grid</b>	<b>Refined grid</b>
Total number of elements	6113	6502
Total number of computational nodes	17600	17989
Number of triangular elements	1187	1965
Number of quadrilateral elements	4926	4537
Front width of the resulting matrix	407	417

As can be seen in Table 1, the total number of elements in the numerical model has increased from 6113 to 6502 and the total number of computational nodes where the solutions of the computations are provided has increased from 17600 in the original model to 17989 in the refined grid model. No further refinement was attempted because, the bathymetry data used in the model was not changed. There is no incremental benefit in increasing the resolution of the grid beyond certain level when the resolution of the bathymetry data remains unchanged.

#### **Updating of the model using the refined grid:**

The model of Krishnappan (2011) was reformulated using the refined grid. The reformulated model was then tested against the original model to ascertain the integrity of the model. For this test, the average monthly flow rate tested in the original model was selected. Accordingly, the refined grid model was set up for the average monthly flow rate of 2120 m<sup>3</sup>/s. This flow included the flow through the Edison Sault Electric Company power plant, which was estimated as 576 m<sup>3</sup>/s. Therefore, the flow rate through the upstream boundary of the model was set as 1544 m<sup>3</sup>/s and the flow rate through the power plant was set at 576 m<sup>3</sup>/s. Two more boundary conditions are needed to run the model. One for the boundary in the navigational channel and the other for the boundary at the downstream end of the computational domain in the main river. Neither the flow rate data nor the water surface elevation data is available for these two boundaries. Therefore, Krishnappan (2011) used a nested modelling approach to resolve this issue. As per this approach, a very coarse grid model developed by United States Army Corps of Engineers (USACE) for the entire St. Mary's River was used to solve for flow and water surface elevation at the boundaries of the present model. A brief outline of the model of USACE is given here for the sake of completeness.

The model of USACE was developed in 2003 to investigate the impact of a dredging project on water levels and flows in the St. Mary's River (Aaron Thompson, ECCC). The coverage of the model is shown in Fig. 3. As can be seen in Fig. 3, the model covers the whole of the St. Mary's

River. The model of USACE was run with the same monthly average flow rate of  $1544 \text{ m}^3/\text{s}$  at the upstream boundary and  $576 \text{ m}^3/\text{s}$  at the power plant. For the downstream boundaries, the flow stages measured at Thessalon, Slab Dock and Rock Cut Channel gauging stations in the St. Mary's River system were used. Since the objective of the model is to predict the flow rate and water levels for the entire river, the elements used in this model are very coarse and hence this model is not suitable for predicting the finer flow details such as flow reversals and re-circulating eddies in the upper part of the St. Mary's River, especially in the areas near BMP and EBMP.

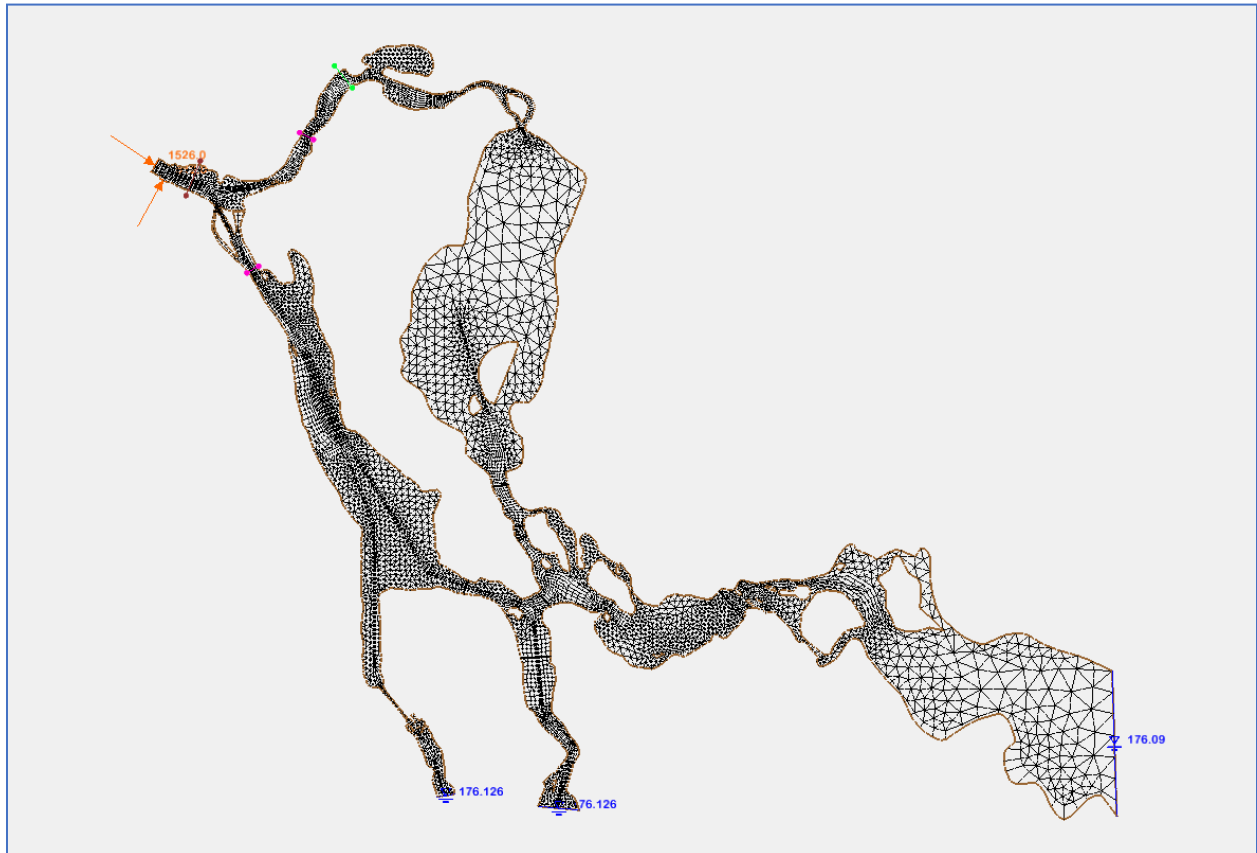


Fig. 3. The coverage of the coarse grid model.

From the output of the USACE model, the flow rate through the Navigation channel and the flow stage at the downstream boundary of the refined grid model were calculated as  $1560 \text{ m}^3/\text{s}$  and  $176.50 \text{ m}$  respectively. Using these values as the remaining boundary conditions, the refined grid model was executed and the results were compared with those of the original model.

Fig. 4. Shows the colour contours of the velocity magnitude predicted by the fine grid model and the Fig. 5 shows the same predicted by the original model.

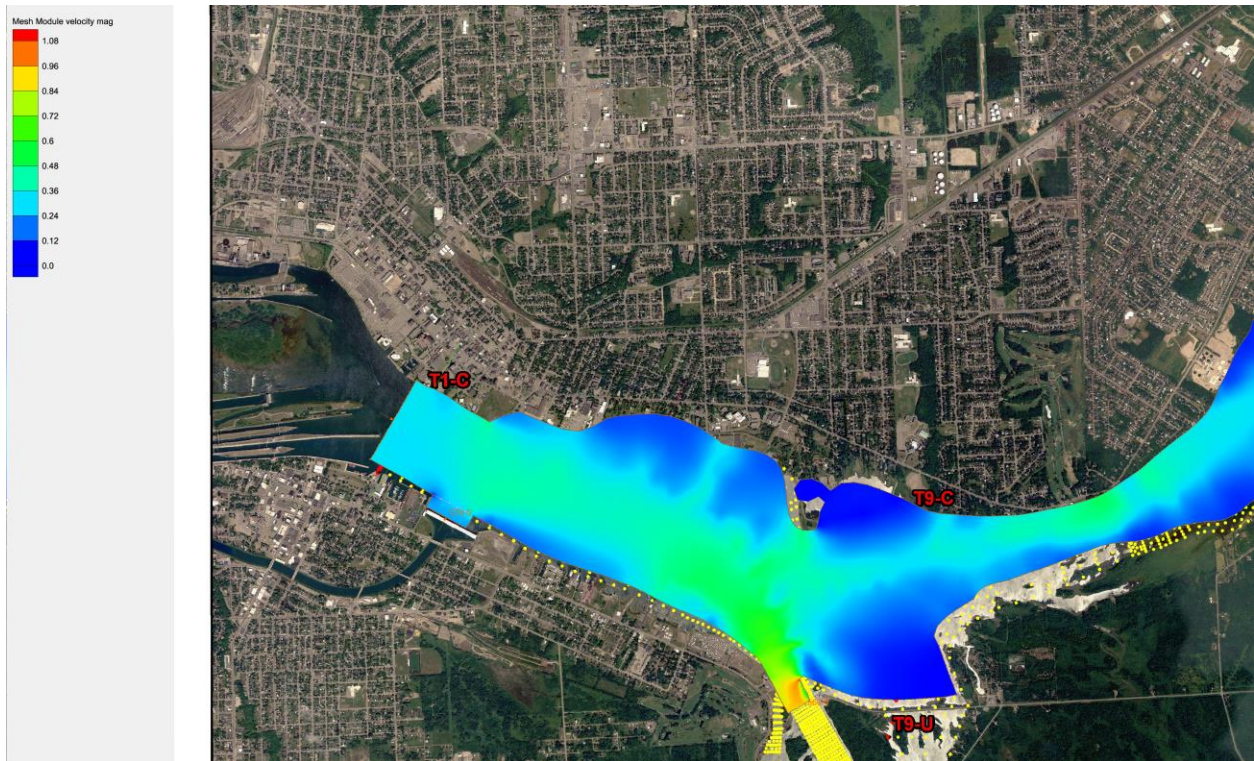


Fig. 4. The colour contours of velocity magnitude as predicted by the refined grid model.

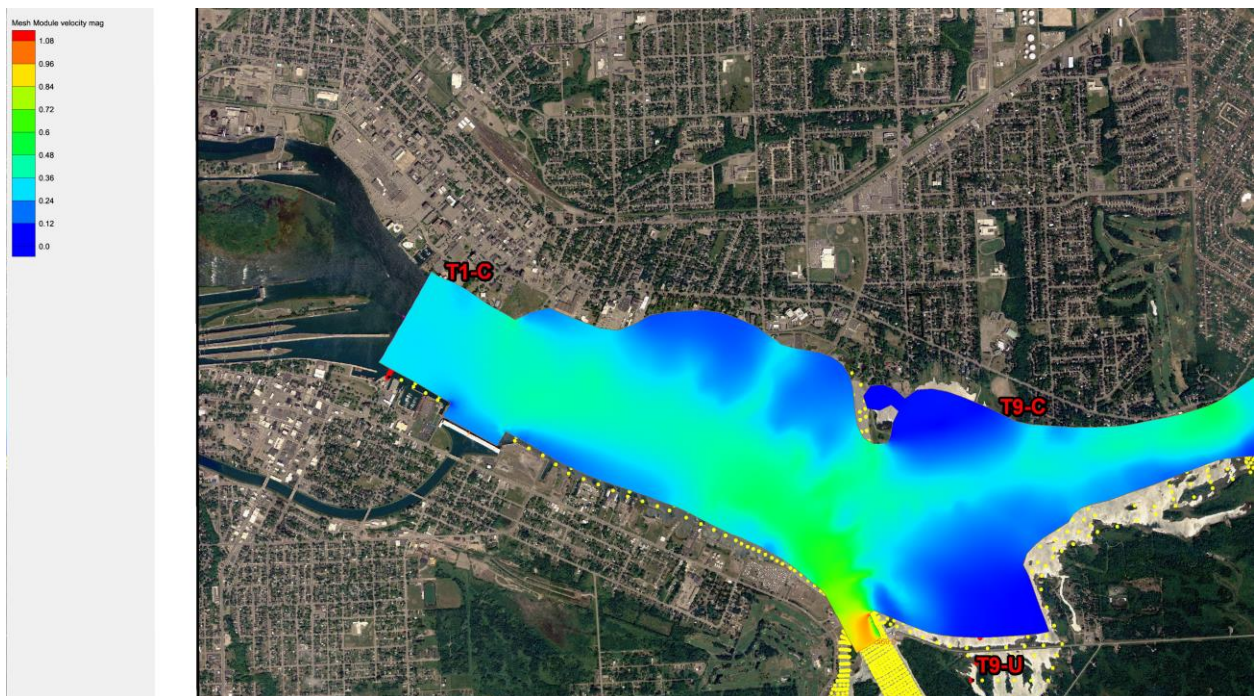


Fig. 5. The colour contours of velocity magnitude predicted by the original model.

By comparing the colour patterns in these two figures, we can see that the predictions of both models are similar. The bed shear stress distributions predicted by both models are shown in Figs. 6 and 7.

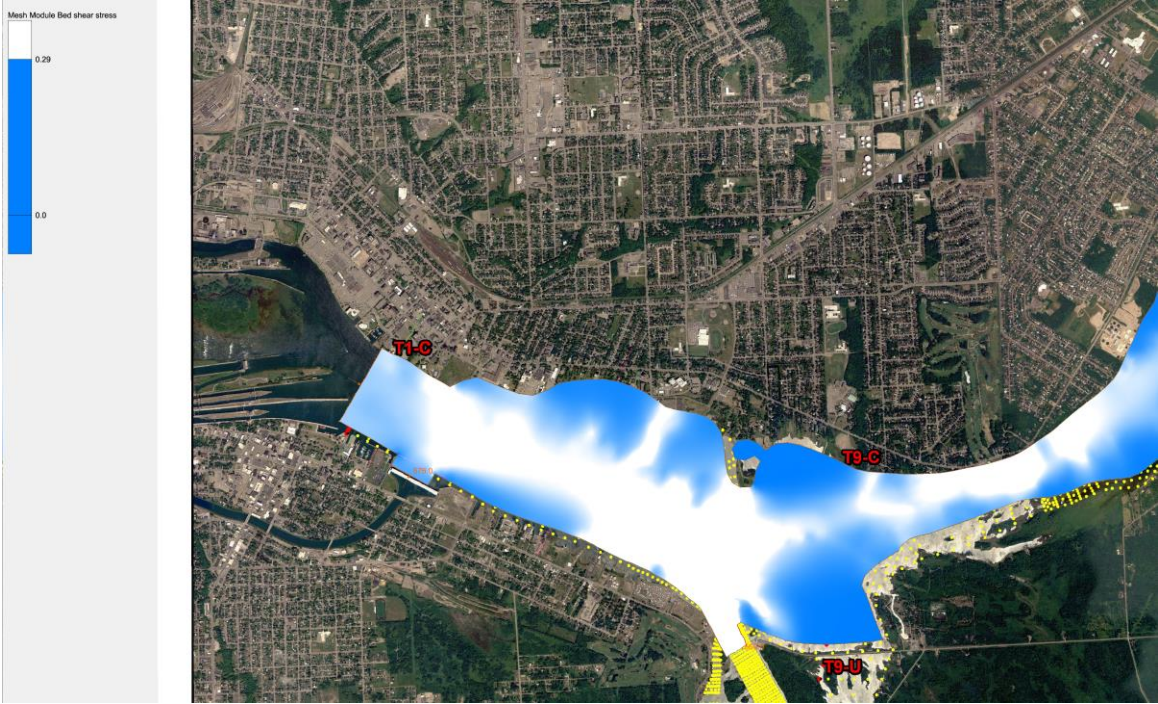


Fig. 6. Bed shear stress distribution predicted by refined grid model.

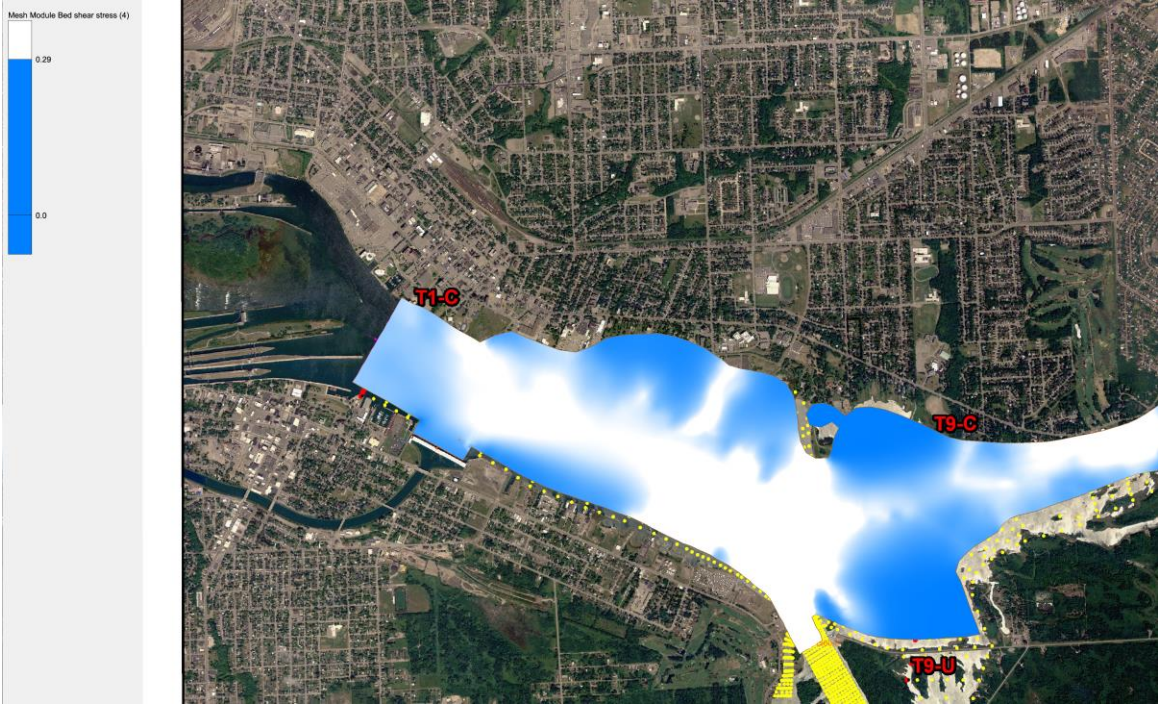


Fig. 7. Bed shea stress distribution predicted by the original model.

In figs. 6 and 7, the shear stresses were considered in two ranges, namely, 0 to 0.29 Pa and above 0.29 Pa. The value of 0.29 Pa was found to be the critical shear stress for erosion of sediment deposits 5 cm below the fluff layer in Krishnappan (2011). From these two figures, it can be seen that the stable region (where shear stress less than 0.29 Pa) exhibits a similar pattern. The velocity vectors predicted by both models are shown in Figs. 8 and 9.

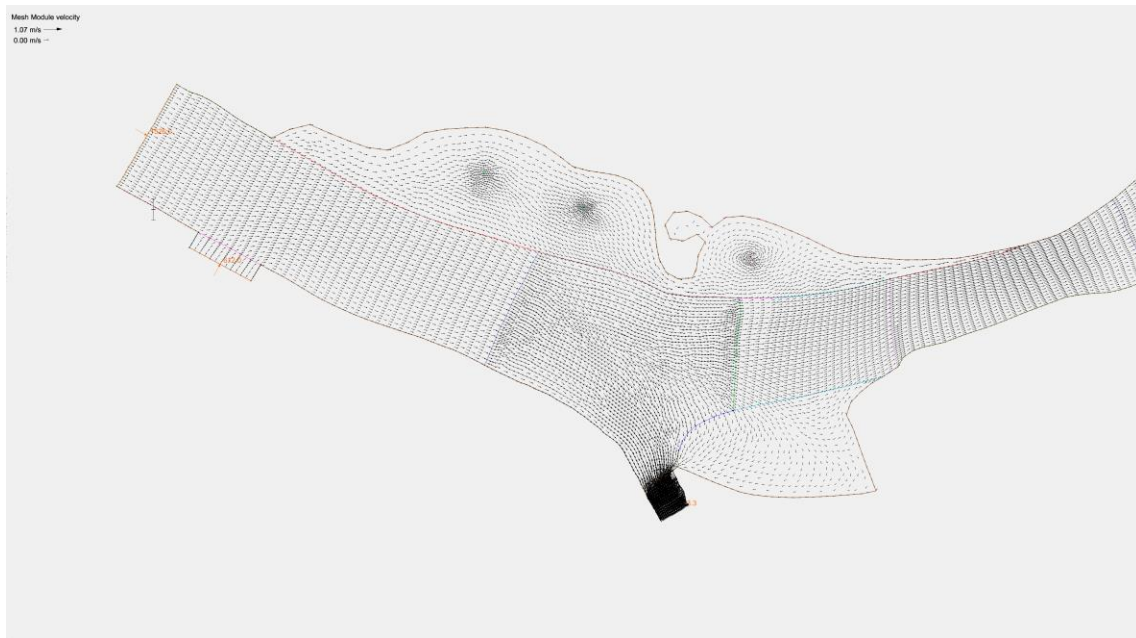


Fig. 8. Velocity vectors predicted by the refined grid model.

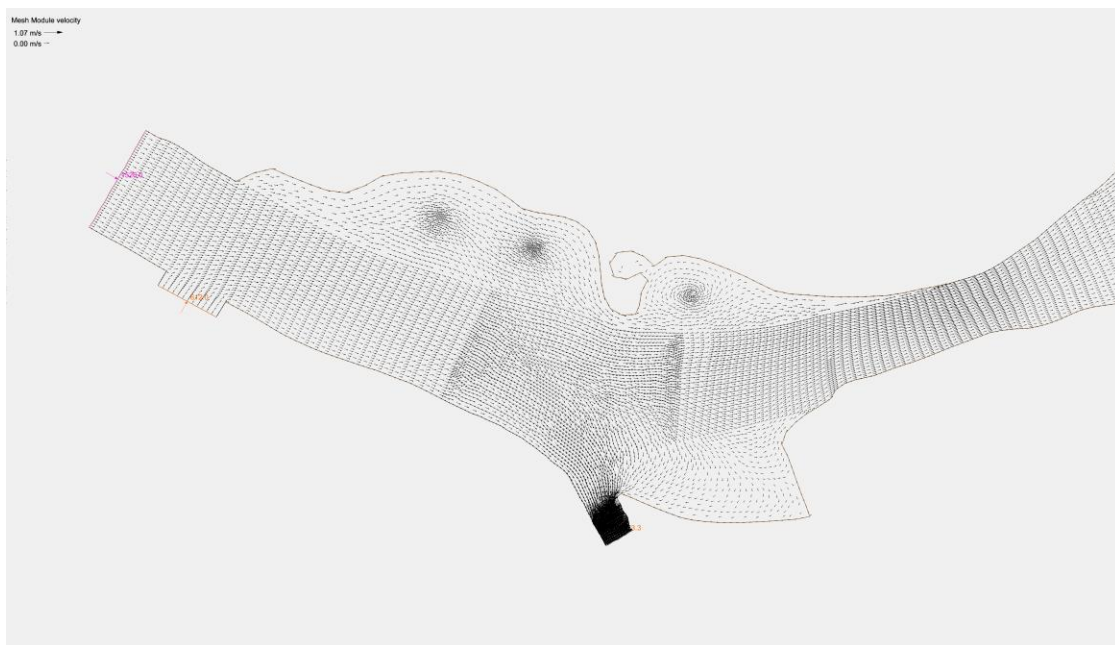


Fig. 9. Velocity vector predicted by the original model.

From Figs. 8 and 9, we can see that the predicted velocities from both models are practically identical. Figs 10 and 11 show the flow traces predicted by both models.



Fig. 10. Flow trace predicted by the refined model.

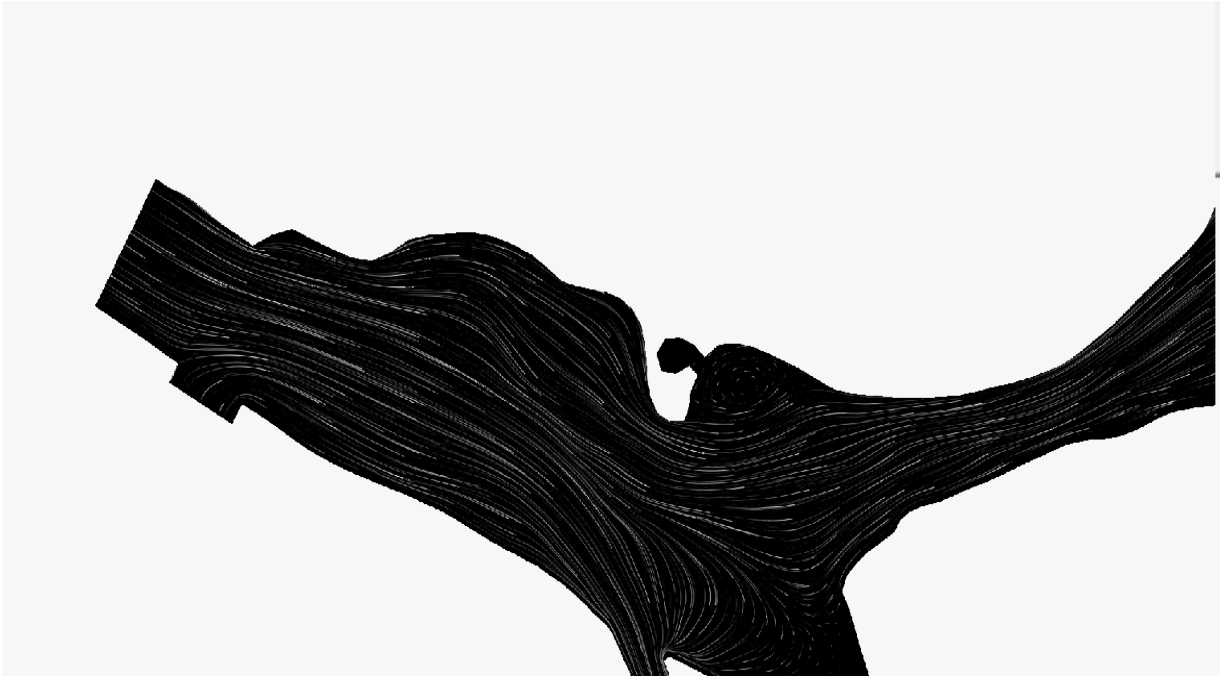


Fig. 11. Flow trace predicted by the original model.

From Figs 10 and 11, we can see that the flow traces predicted by both models are also very similar. From these qualitative comparisons shown in Figs. 4 to 11, it can be concluded that the refined grid model was assembled correctly and it works as well as the original model.

To provide a quantitative comparison between the predictions of both models, three different transects were selected in the study region as shown in Fig. 12.

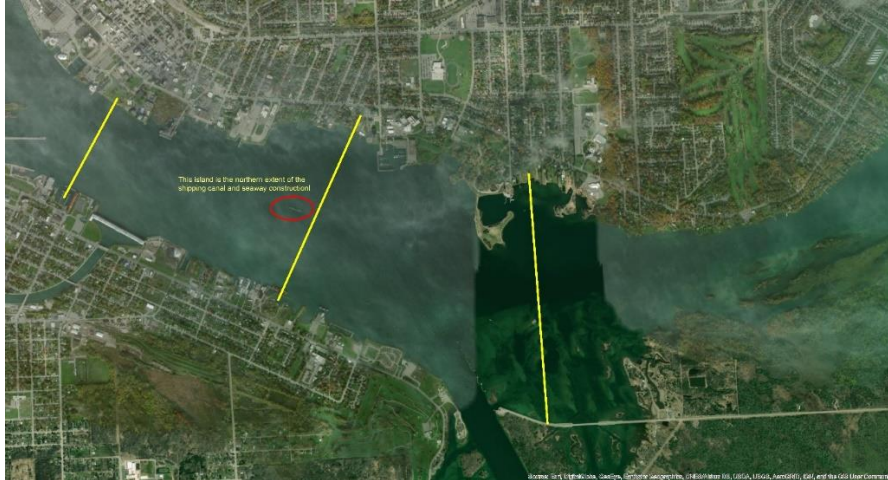


Fig.12. An image with three transects selected for model comparison (Image provided by Hans Biberhofer of ECCC).

The image in Fig. 12 was imported into the SMS model by georeferencing the image with the UTM coordinates projection used in the model. By superimposing the three transects with the model grid, the solutions of the model at these three transects can be extracted. The integration of the image with the transects and the SMS model grid is shown in Fig. 13.

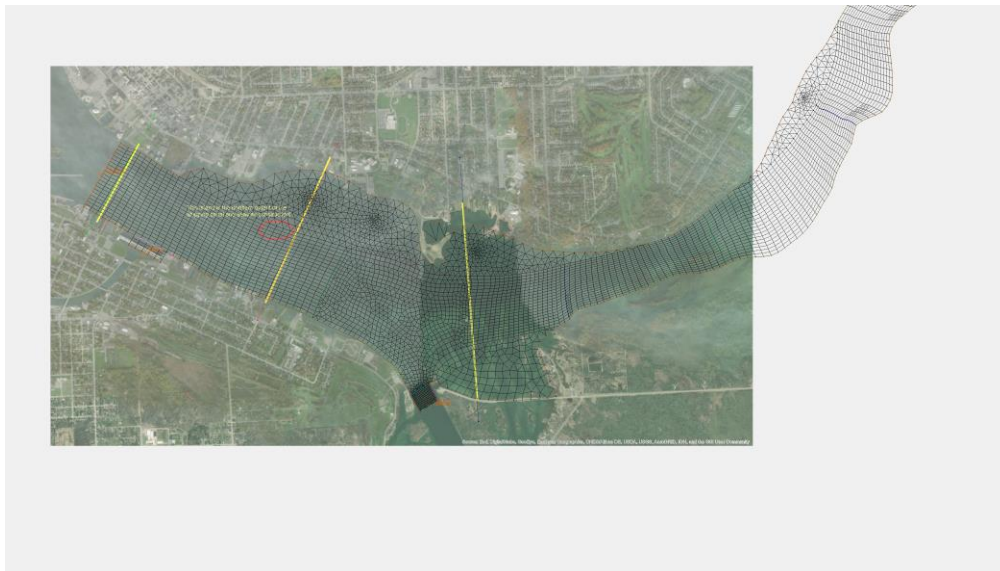


Fig. 13. The integration of the image with the transects and the SMS model grid.

A feature in the SMS model that allows the control of the transparencies of the imported image and the displayed model results facilitates the superposition. The velocity magnitude data for these three transects are shown in Fig. 14. The left most transect was at the entrance of the river and it is designated as the River Inlet. The middle transect was designated as the BMP transect and the right most transect was designated as the EoT transect. The solid lines in Fig. 14 are the velocity magnitude predicted by the original model and the points represent the velocity predictions of the Refined grid model. As can be seen from Fig.14, the velocity predictions of both models match very well and hence it can be concluded that the refined grid model was implemented correctly. Since the refined grid model contains higher number of computational nodes in the BMP and EBMP areas, it is expected that the refined grid model predictions will of higher resolution in these regions.

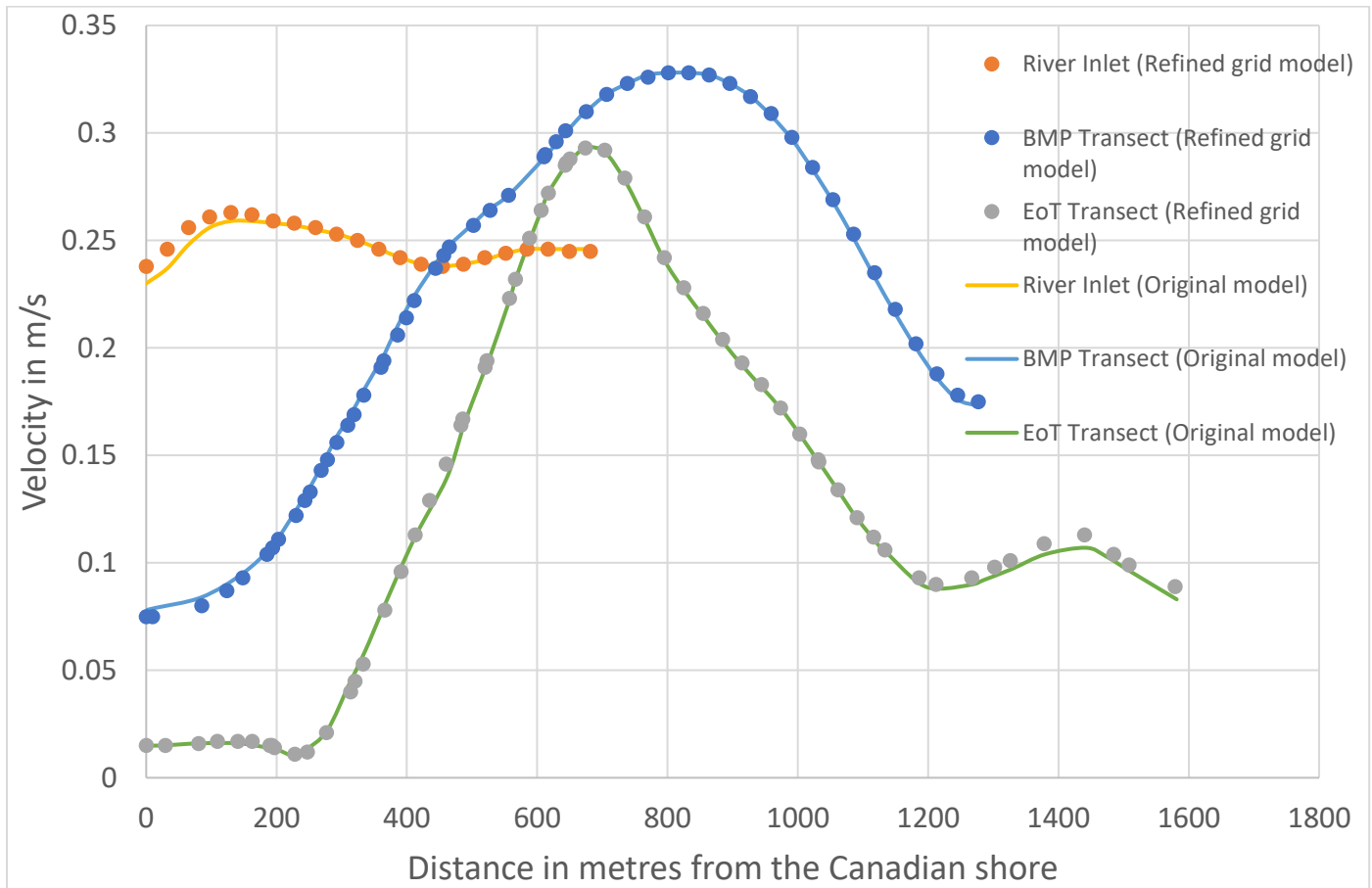


Fig. 14. Velocity distributions predicted by the Refined grid model and the original model at the selected transects for the average flow conditions tested.

### Updating of the background image for the SMS model:

The background image registered in the original SMS model grid covers the entire model domain, but it suffers from low resolution and hence it was not georeferenced accurately. As a result, some portion of the grid overlapped the land area. To overcome this drawback, a high resolution image (provided by Hans Biberhofer of ECCC) was used as a background image for the refined grid model. The image used in the refined model is shown in Fig. 15.

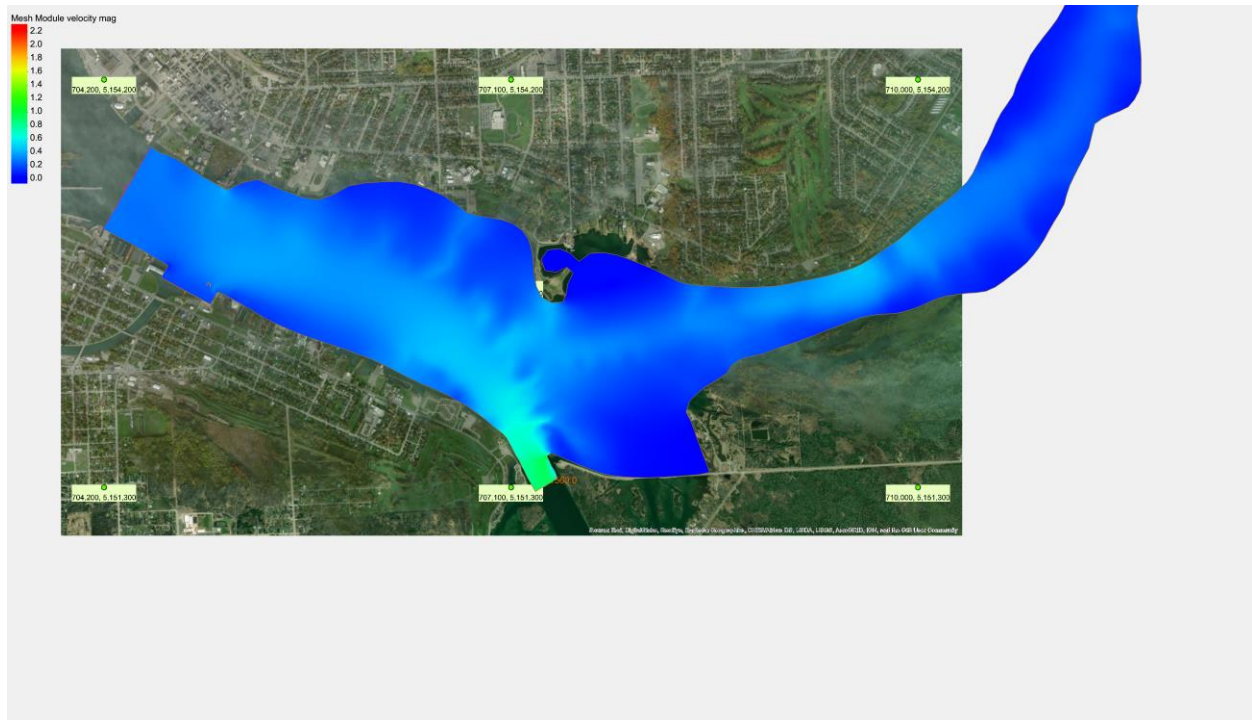


Fig. 15. New background image (provided by Hans Biberhofer) used in the refined grid model in SMS.

The new image shown in Fig. 15 covers the BMP and EBMP areas including the area east of Top Sail Island. With this image, the grid boundaries followed the shorelines better indicating that the georeferencing of the image was more accurate than with the previous image. With this image, it is possible to superimpose the measured data in the field with the model predictions of hydrodynamic properties in the river. As an example, Fig. 16 shows an overlay of sediment deposition area East of Top Sail Island with the velocity vector distribution predicted by the model for average flow conditions in the river. Similar comparisons are possible by georeferencing the images that contain measured information in the field in terms of the model grid coordinates and superimposing them on the model predictions by adjusting the transparencies of both.

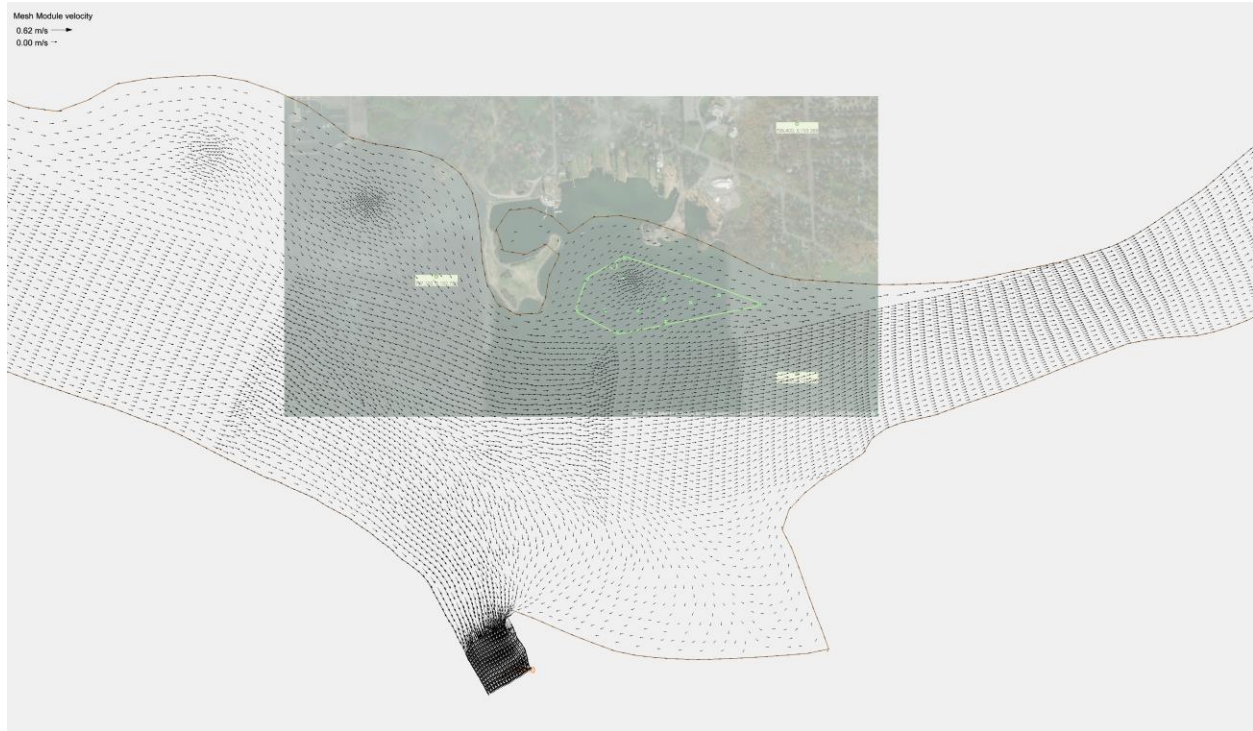


Fig. 16. Superposition of sediment deposition area with the velocity field generated by the refined grid model for the average flow conditions in the river.

### Testing of flow scenarios:

The refined grid model was used to predict the flow properties in the St. Mary's River using the daily discharge data for the River. The period of record of available data for the river covers from April 2002 to present. The daily average discharge data for the period from April 2002 to March 2021 is plotted in Fig. 17. From this figure, it can be seen that the maximum flow rate occurred on August 6<sup>th</sup> of 2005 with a flow rate of 3657 m<sup>3</sup>/s, and the minimum flow rate occurred on April 12<sup>th</sup> of 2009 with a flow rate of 887 m<sup>3</sup>/s. The data in Figure 17 also shows that there is a shift in the flow regime in the river. Prior to 2014, the flow rates on average are lower in comparison to flow rates after the year 2014.

A flow duration analysis showed that the flow regime indeed had shifted after 2014. The flow duration analysis carried out for the flow record prior to 2014 and that for the record after 2014 are compared in Figure 18 along with the analysis for the entire record. It can be seen from Fig. 18 that the flow duration curve had shifted upwards for the records after 2014 in comparison to the record prior to 2014 and for the full record. For the probability of exceedance of 0.5, which means that 50% of the time the flow rate had exceeded the given value has changed from 1780 m<sup>3</sup>/s to 2440 m<sup>3</sup>/s.

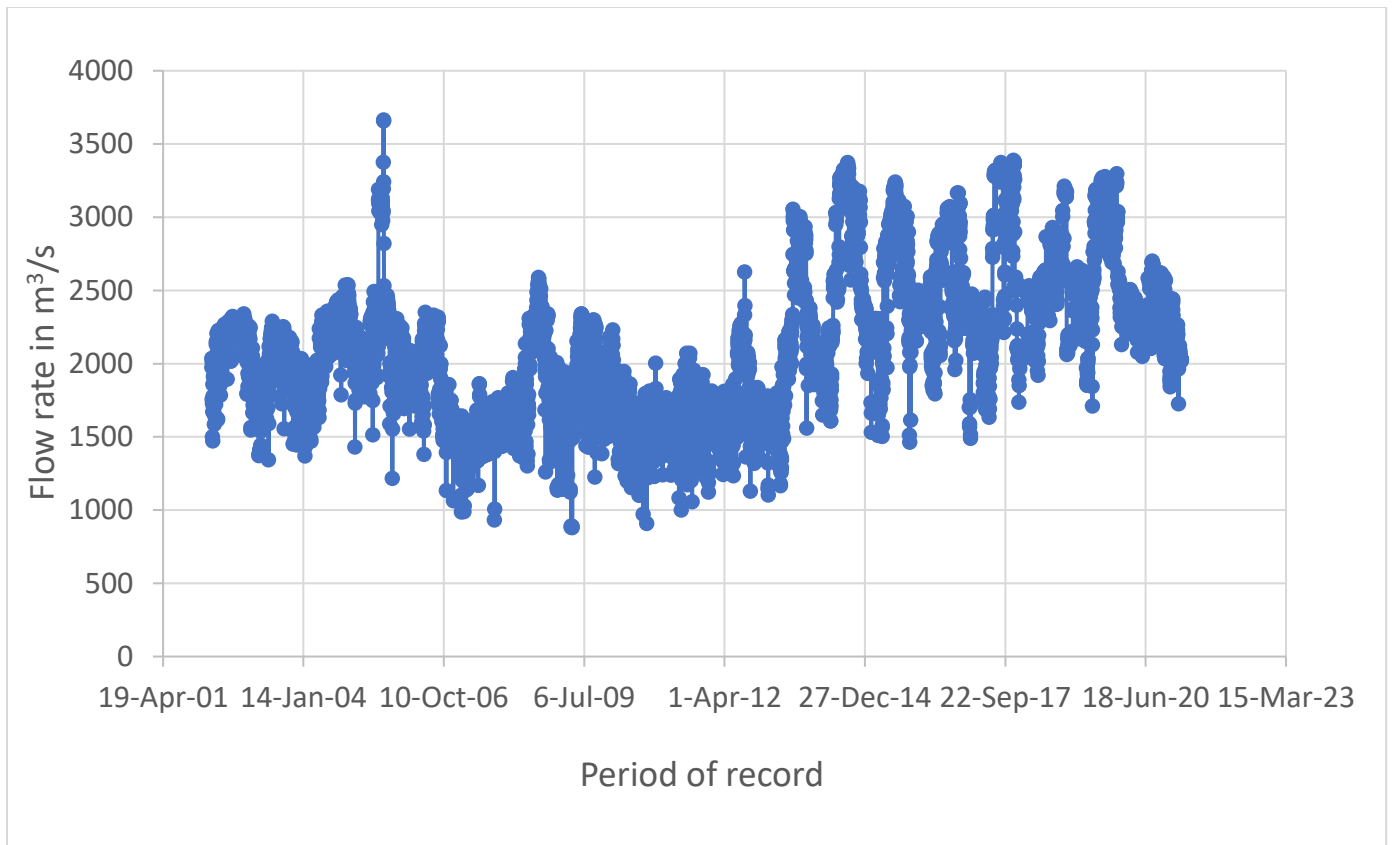


Fig. 17. Daily average discharge data for the St. Mary's River from April 2002 to March 2021.

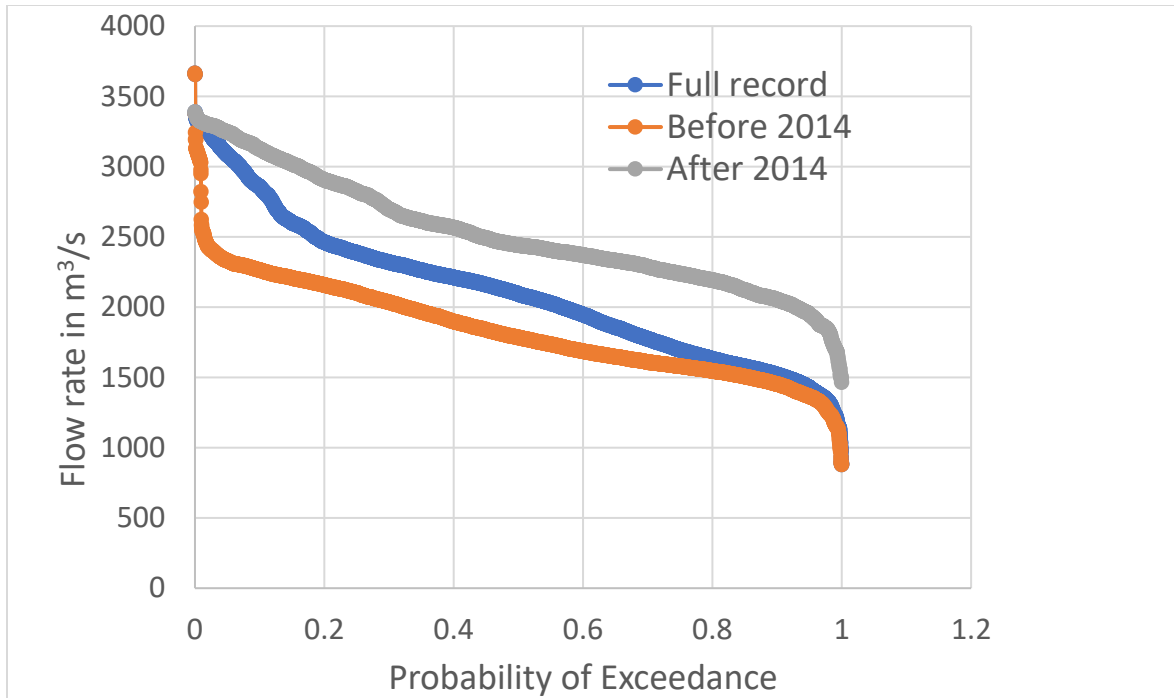


Fig. 18. Flow duration curves for different period of records of flow data for the St. Mary's River.

Based on the flow records and the flow duration analysis, the following flows were selected for simulation with the refined grid model.

Table 2. Flow rates selected for simulation using the refined grid model.

Flow rate with the probability of exceedance of 0.5 (i.e., 50% of the time this flow rate has been exceeded).	2440 m <sup>3</sup> /s
Maximum recorded daily discharge on August 6, 2005	3657 m <sup>3</sup> /s
Maximum flow that can be physically released.	4300 m <sup>3</sup> /s

The Maximum flow rate that can be physically released was included in the modelling scenarios to examine the worst-case scenario.

In addition to the flow records for the river, the flow rates released from the hydroelectric power plant downstream of the river inlet are also needed for the model simulations. The flow data was obtained from the Cloverland Hydro Electric Cooperative formerly know as the Edison Sault Electric Company for the period from January 2000 to present. The data is plotted in Fig. 19.

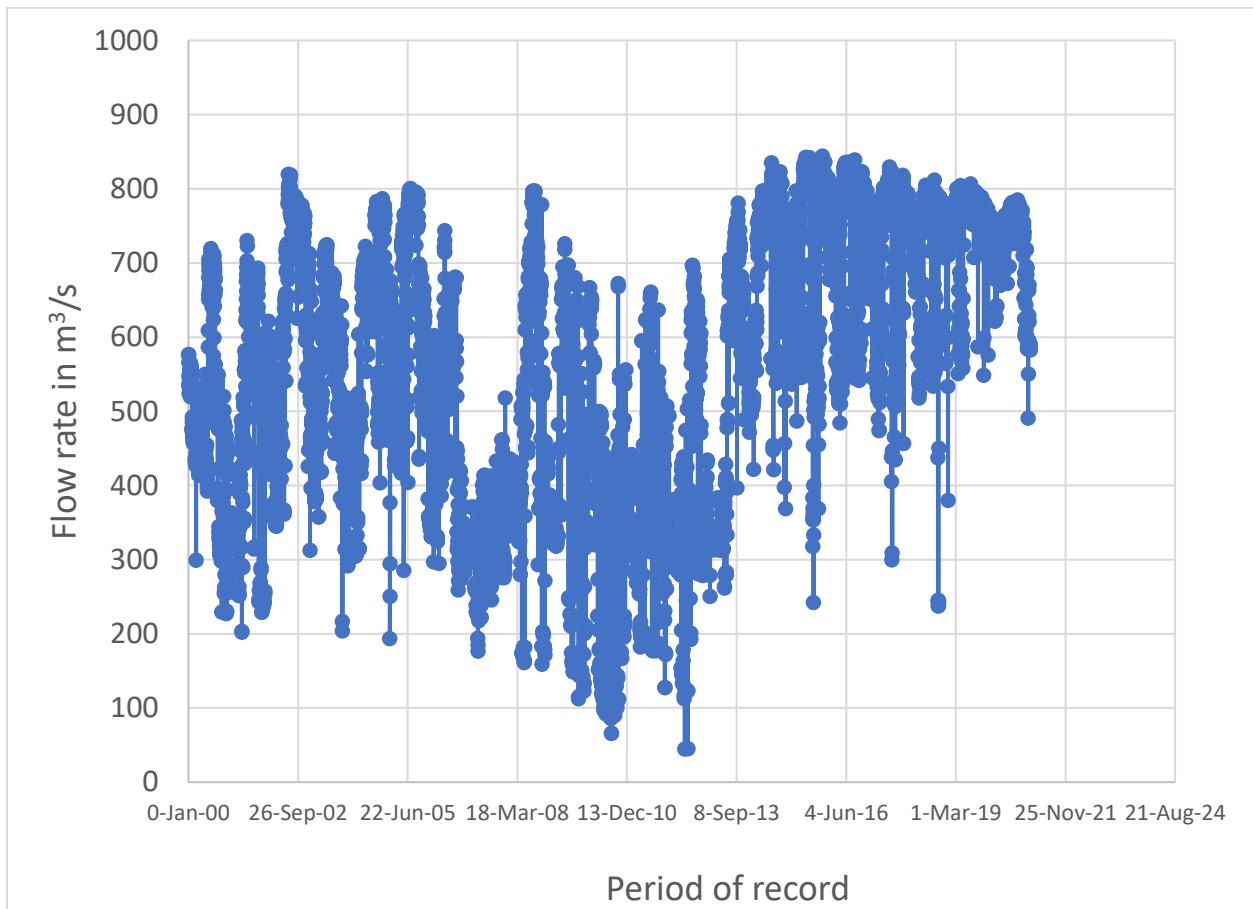


Fig. 19. Daily average discharge data from the Cloverland Electric Cooperative

The flow records in Fig. 19 shows three distinct flow groups. The first group which spans from Year 2000 to Year 2007 has an average flow rate of 549 m<sup>3</sup>/s. The middle group spanning Year 2007 Year 2014 has an average flow rate of 413 m<sup>3</sup>/s and the third group from Year 2014 to present has an average flow rate of 708 m<sup>3</sup>/s. For the present simulation using the 50% exceedance flow rate of 2440 m<sup>3</sup>/s, the average flow rate from the third group of 708 m<sup>3</sup>/s was used. For the simulation of the maximum flow rate of 3657 m<sup>3</sup>/s, the actual flow rate that was measured on the 6<sup>th</sup> August 2005 (namely, 783 m<sup>3</sup>/s) was used. For the worst-case scenario flow of 4300 m<sup>3</sup>/s, a maximum flow rate of 867 m<sup>3</sup>/s which was measured during September 1985 (see Krishnappan (2011)) was used.

### Results from the 2440 m<sup>3</sup>/s flow simulation:

The boundary conditions used for this simulation are as follows: Flow rate at the river inlet is 1732 m<sup>3</sup>/s and the flow rate from the Cloverland hydroelectric power plant is 708 m<sup>3</sup>/s to give a total flow of 2440 m<sup>3</sup>/s in the river downstream of the power plant. The flow rate through the navigation channel and the water surface elevation at the downstream boundary of the model domain, which is located just upstream of Little Lake George were calculated using the USACE model as described earlier. The values obtained were as follows: the flow rate through the navigation channel was 1798 m<sup>3</sup>/s and the water surface elevation at the downstream boundary of the model domain was 176.42 m. Using these boundary conditions, the refined grid model was run and the flow properties predicted by the model are presented in what follows next.

Fig. 20 shows the magnitude of the velocity vector predicted by the model.

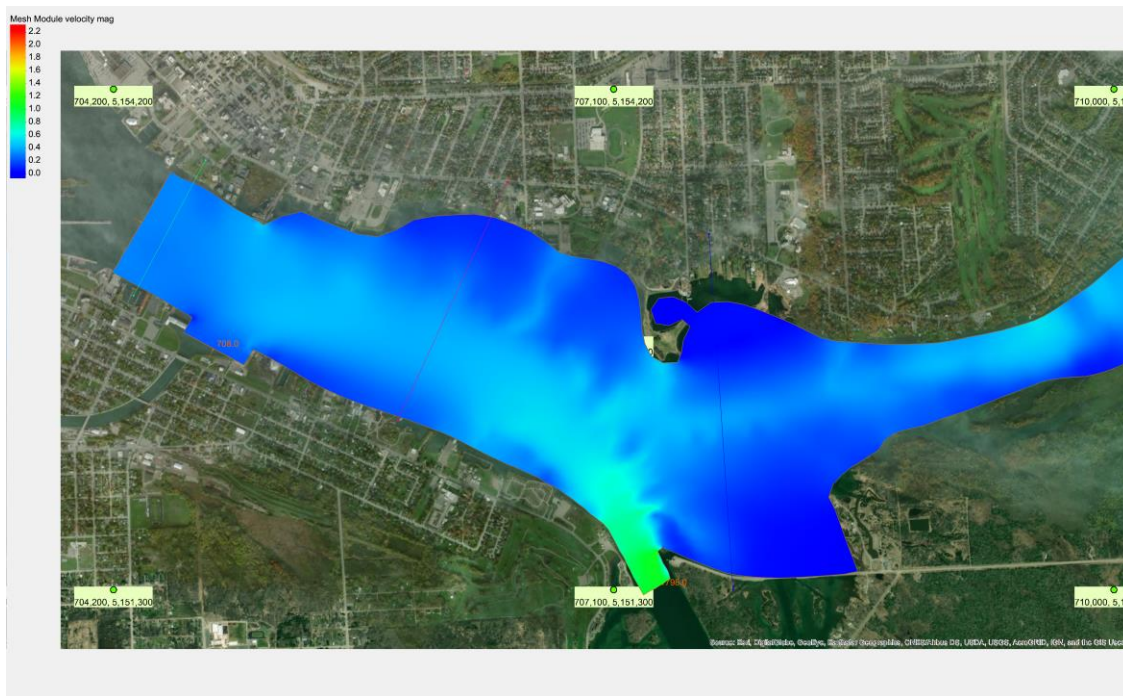


Fig. 20. Velocity magnitude predicted by the refined grid model for flow rate of 2440 m<sup>3</sup>/s.

The bed shear stress distribution predicted by the model is shown in Fig. 21.

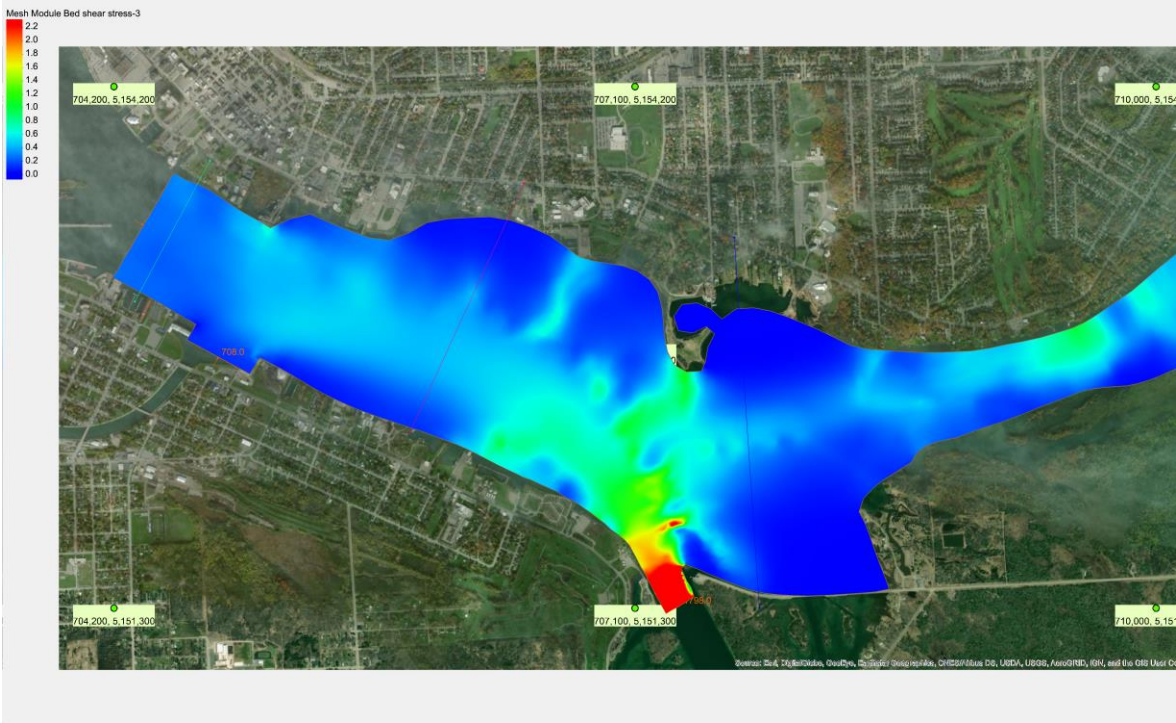


Fig. 21 Bed shear stress distribution predicted by the refined grid model for the flow rate of 2440 m<sup>3</sup>/s.

The velocity vector plot for the run is shown in Fig. 22.

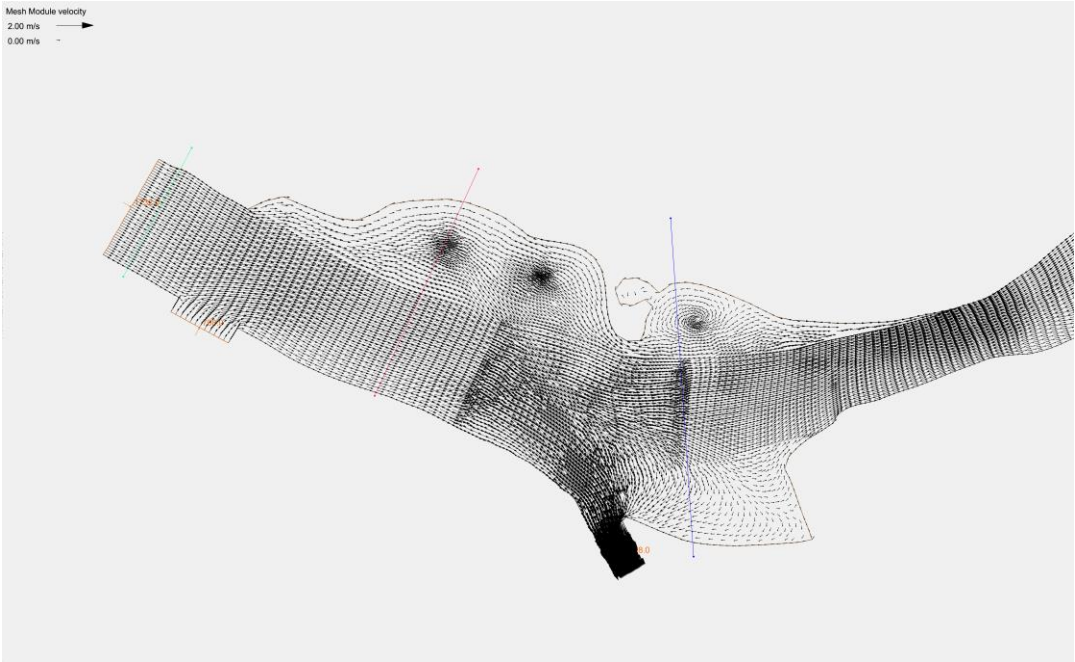


Fig. 22 Velocity vectors predicted by the refined grid model for the flow rate of 2440 m<sup>3</sup>/s.

The velocity magnitude and beds shear stress variations across the river at selected transect are shown in Figs. 23 and 24 respectively. The selected transects are the same ones shown in Fig. 12.

### Distribution of velocity across the river for the flow rate of 2440 m<sup>3</sup>/s At three selected transects

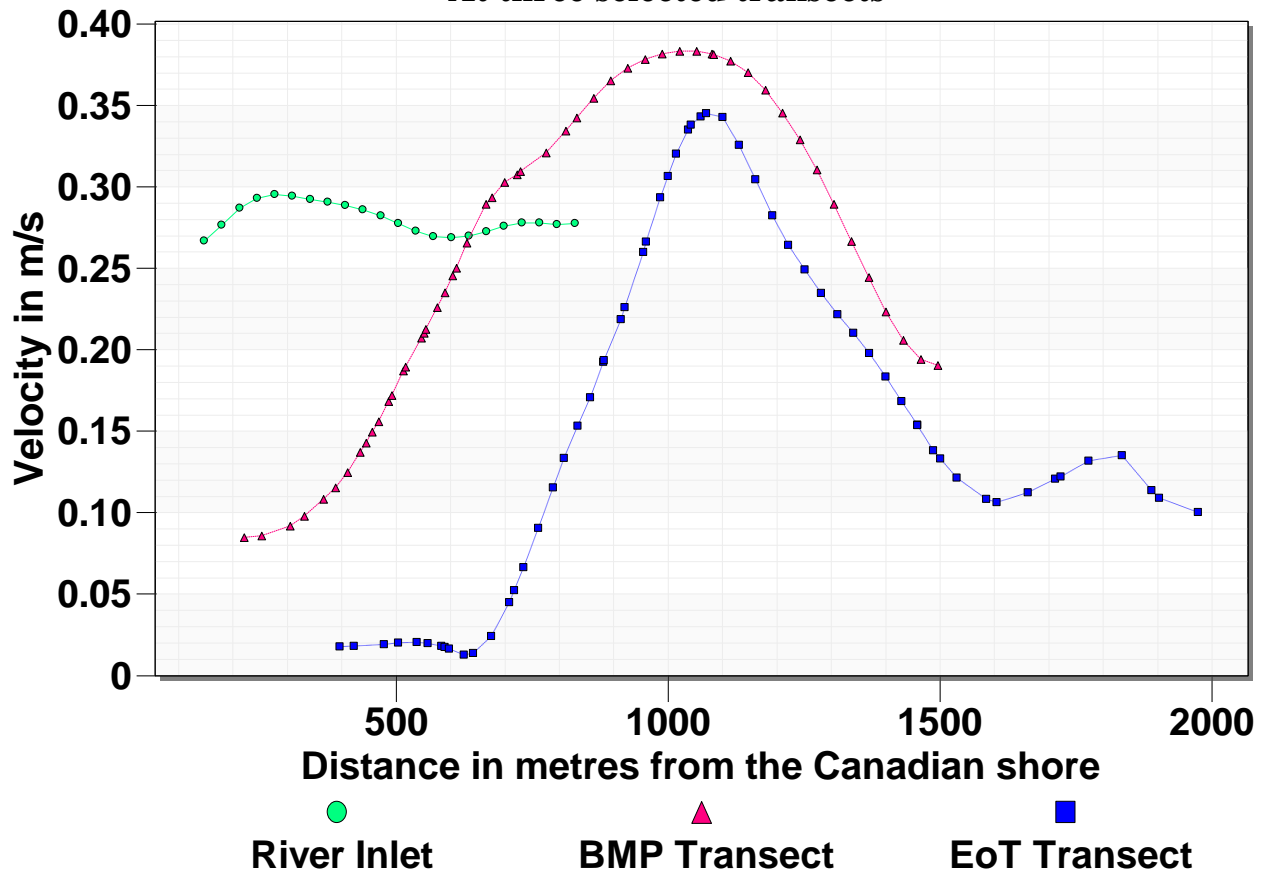


Fig. 23 Velocity distribution predicted by the refined grid model for the flow rate of 2440 m<sup>3</sup>/s at three selected transects.

## Bed shear stress distribution for the flow rate of 2440 m<sup>3</sup>/s At three selected transects

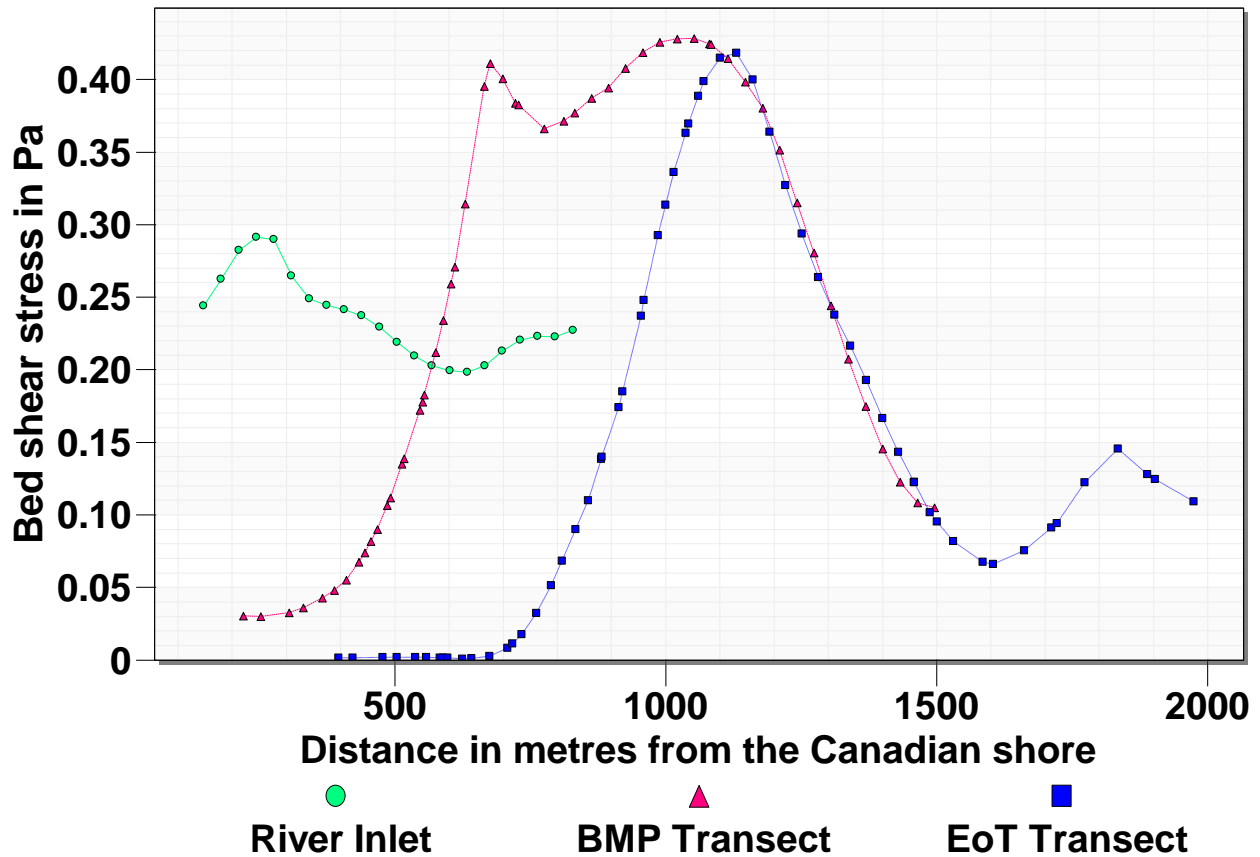


Fig. 24. Bed shear stress distributions predicted by the refined grid model for the flow rate of 2440 m<sup>3</sup>/s at three selected transects.

### Results from the 3657 m<sup>3</sup>/s flow simulation:

For the 3657 m<sup>3</sup>/s simulation, the following boundary conditions were used. The flow rate at the river inlet was 2874 m<sup>3</sup>/s and the flow rate from the hydroelectric power plant was 783 m<sup>3</sup>/s. The flow rate through the navigation channel and the water surface elevation at the downstream end of the model domain were calculated using the USACE model as 2674 m<sup>3</sup>/s and 176.70 m respectively. Using these boundary conditions, the refined grid model was run and the results are presented in the same sequence as was done for the previous flow simulation. As such, the velocity magnitude predicted by the model is shown in Fig. 25, followed by the bed shear stress distribution in Fig. 26, velocity vector plot in Fig. 27, and the velocity and bed shear stress variations across the river at the selected transects in Figs. 28 and 29 respectively.

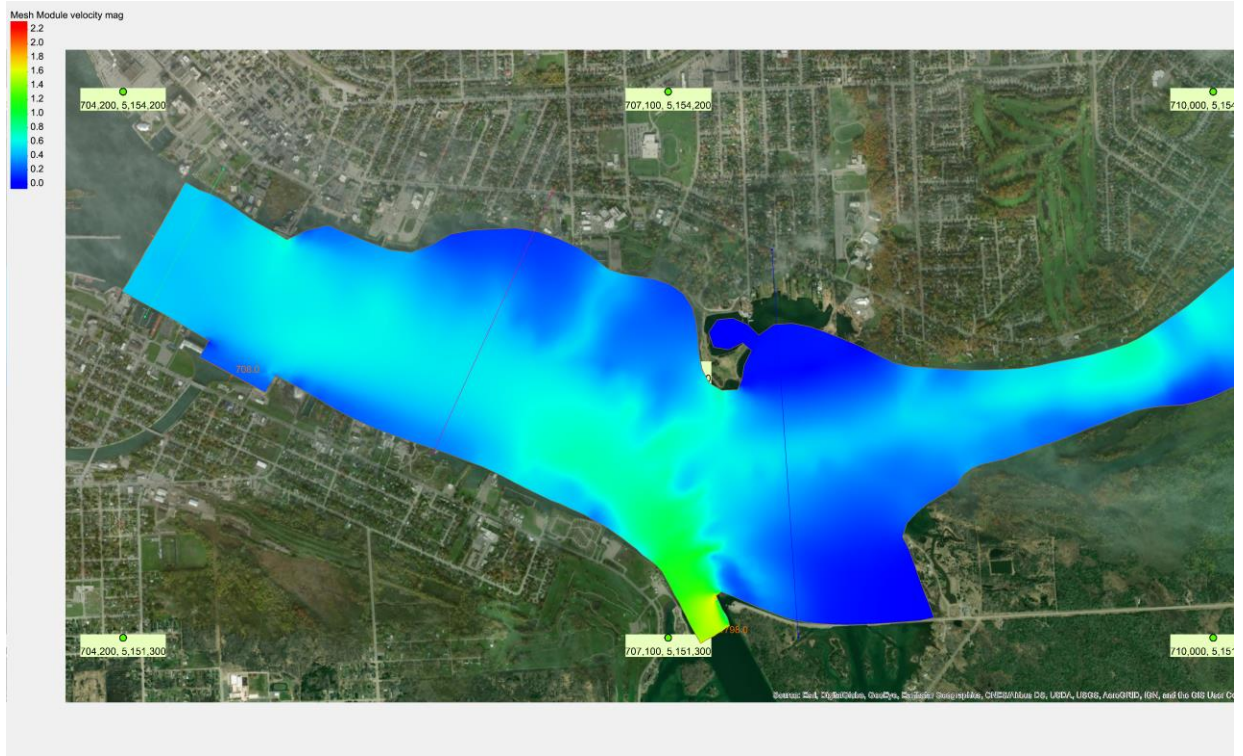


Fig. 25. Velocity magnitude predicted by the refined grid model for the flow rate of 3657 m<sup>3</sup>/s.

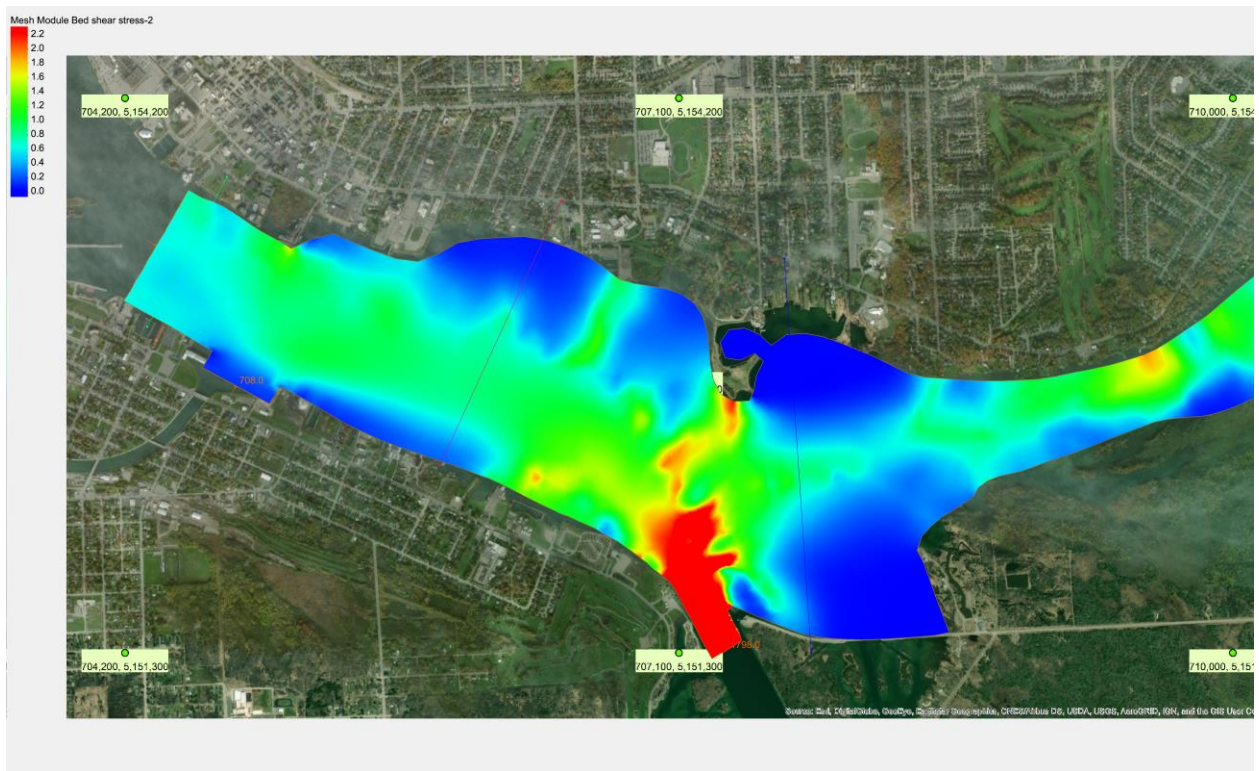


Fig. 26. Bed shear stress distribution predicted by the refined grid model for the flow rate of 3657 m<sup>3</sup>/s

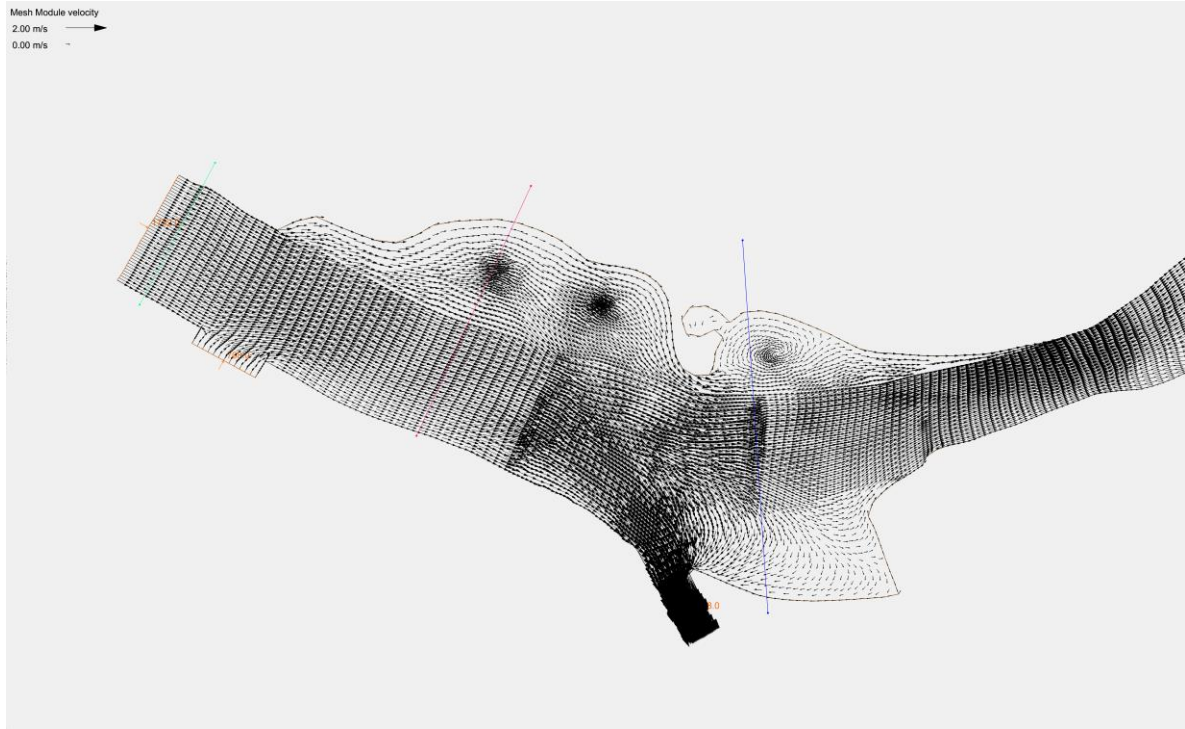


Fig. 27. Velocity vectors predicted by the refined grid model for the flow rate of 3657 m<sup>3</sup>/s.

### Velocity distribution for the flow rate of 3657 m<sup>3</sup>/s

At selected transects

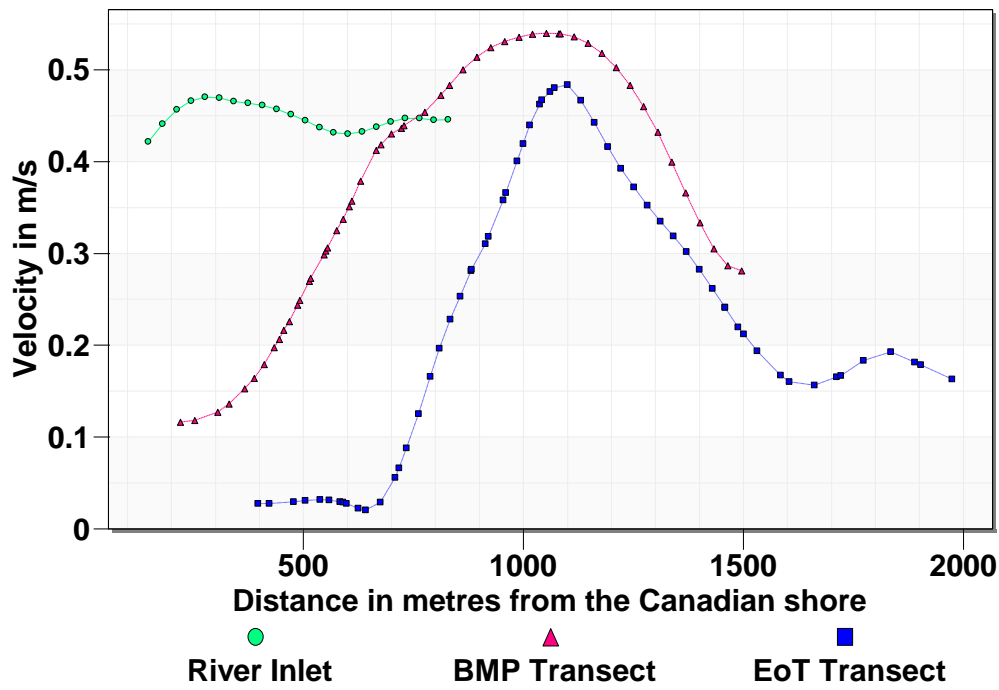


Fig. 28. Velocity variation across the channel at three selected transects for 3657 m<sup>3</sup>/s run.

## Bed shear stress distribution for the flow rate of 3657 m<sup>3</sup>/s A three selected transects

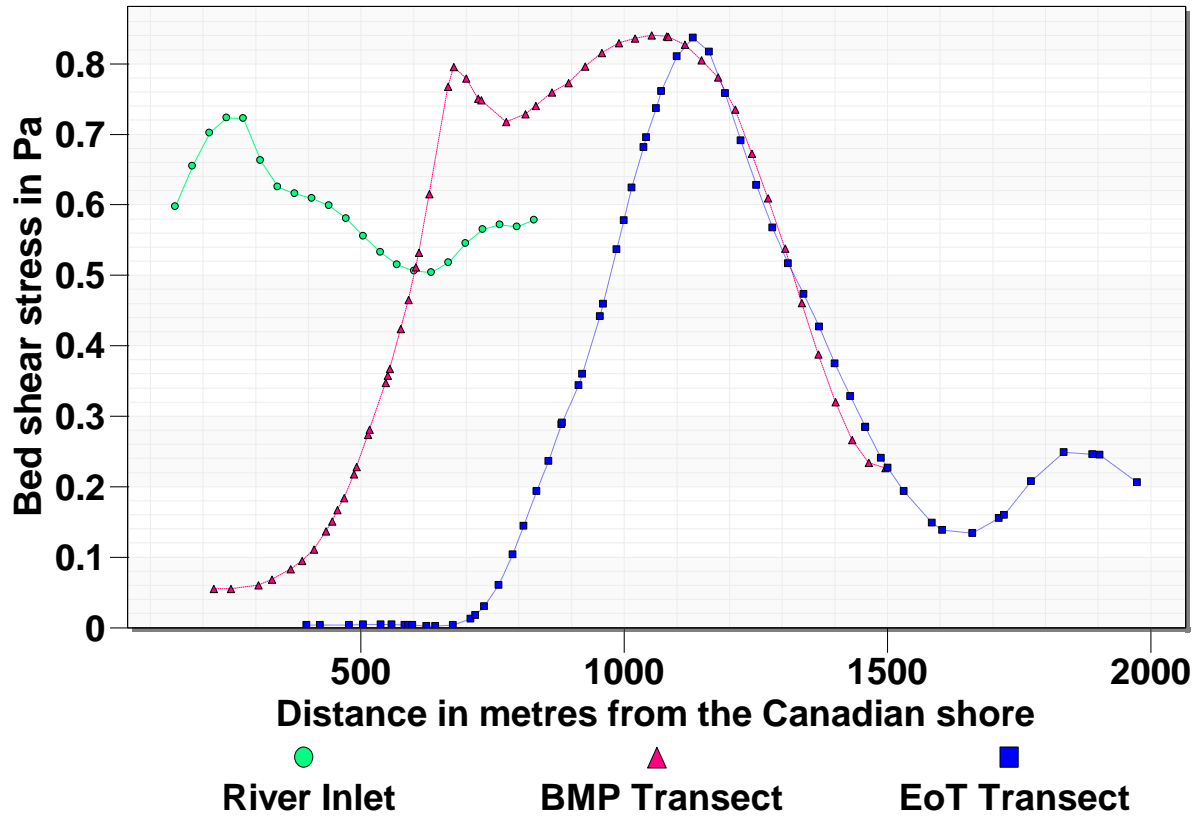


Fig. 29. Bed shear stress variation across the river at three transects for the flow rate of 3657 m<sup>3</sup>/s.

### Results from the 4300 m<sup>3</sup>/s flow simulation:

The boundary conditions used for simulating this maximum flow that can be physically released from the lake are as follows: The flow rate through the river inlet was 3433 m<sup>3</sup>/s, the flow rate through the hydroelectric power plant was 867 m<sup>3</sup>/s, the flow through the navigation channel was 3133 m<sup>3</sup>/s and the water surface elevation at the downstream boundary of the computational domain was 176.875 m. The results from this simulation are presented here in the same sequence as for the previous two flow simulations. Therefore, the velocity magnitude predictions are shown in Fig. 30, the bed shear stress predictions are shown in Fig. 31, The velocity vector plot in Fig. 32 and the velocity and bed shear stress variation across the river at three selected transects in Figs 33 and 34 respectively.

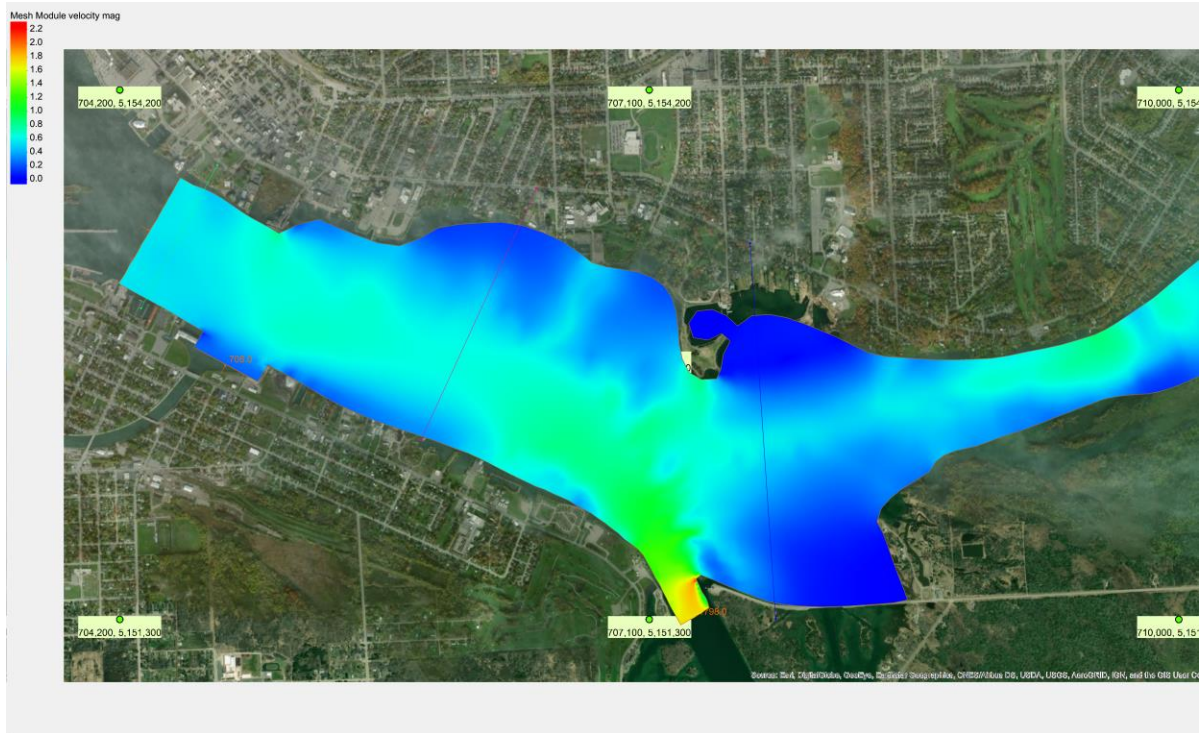


Fig. 30. Velocity magnitude predicted by the refined grid flow model for the flow rate of 4300  $m^3/s$ .

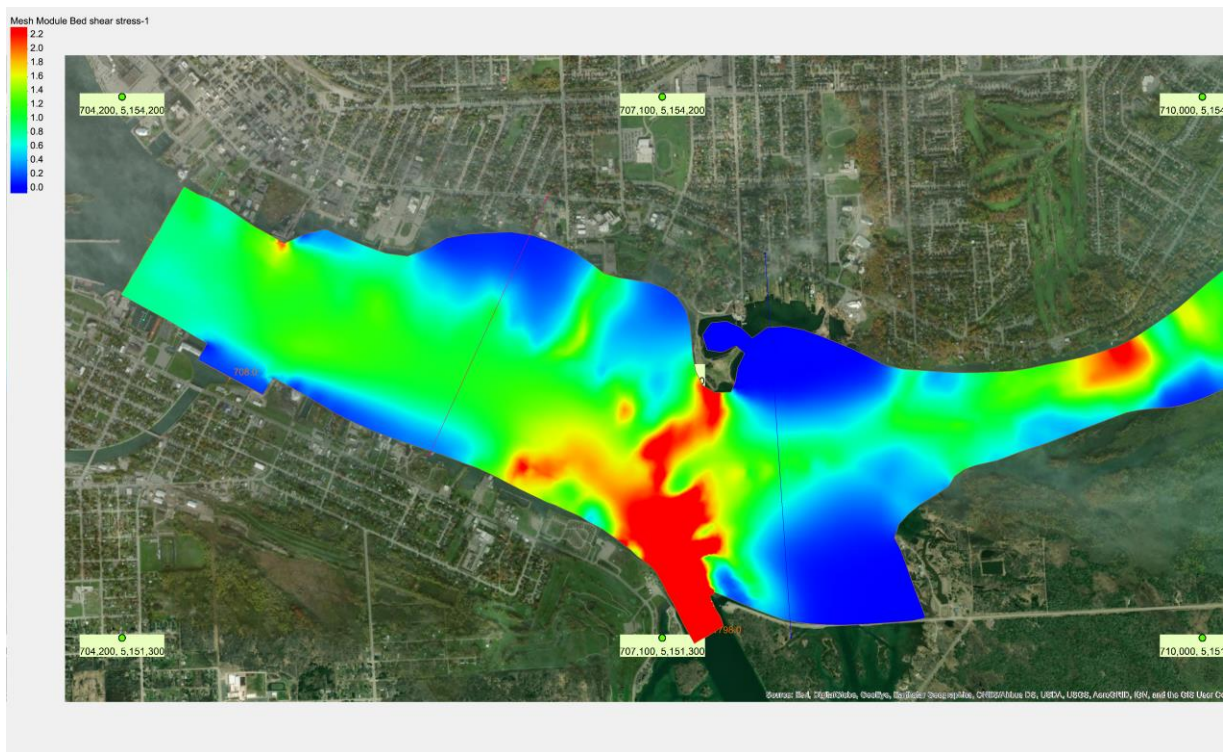


Fig. 31. Bed shear stress predictions by the refined grid flow model for the flow rate of 4300  $m^3/s$ .

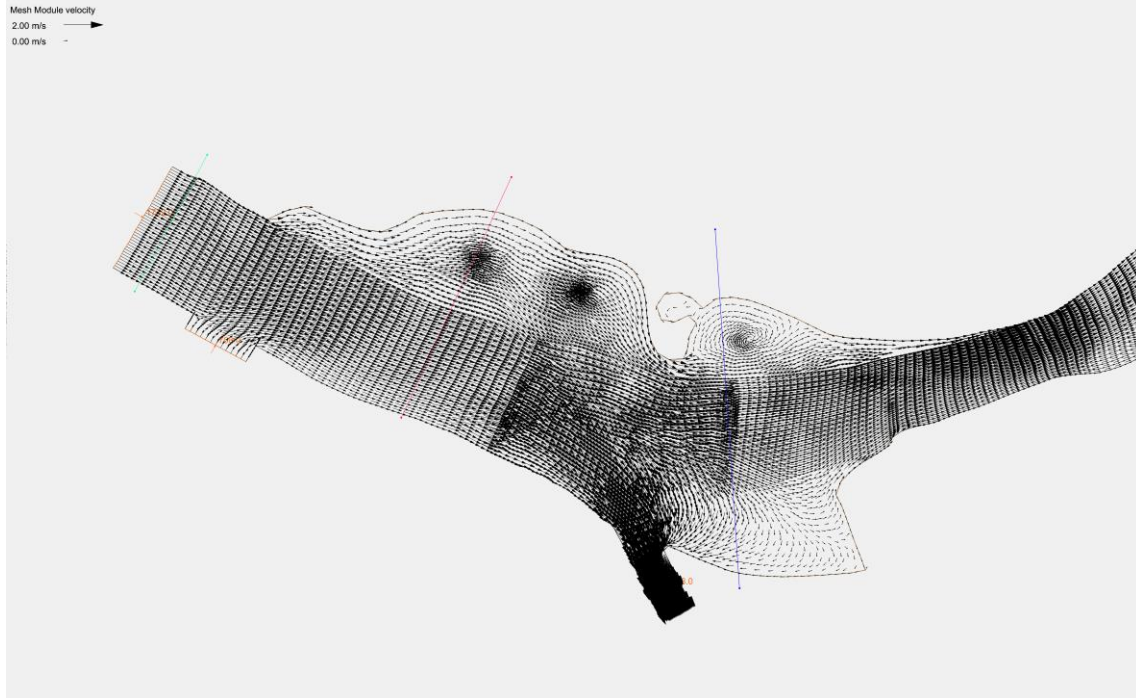


Fig. 32. Velocity vectors predicted by the refined grid model for the flow rate of 4300 m<sup>3</sup>/s.

### Velocity distribution for the flow rate of 4300 m<sup>3</sup>/s At three selected transects

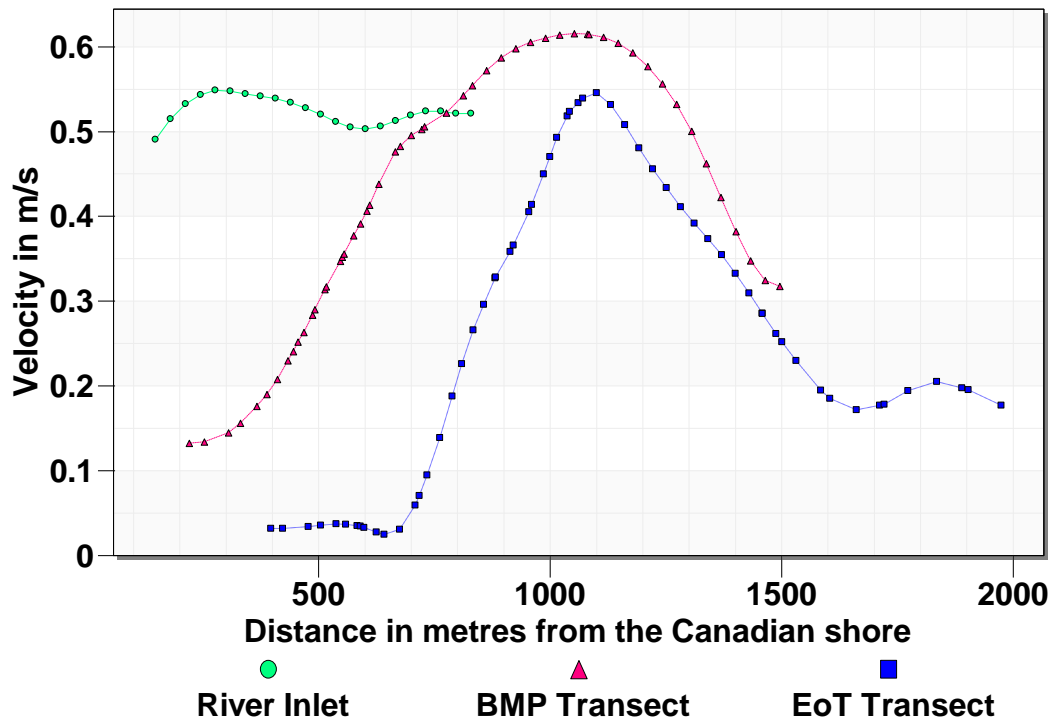


Fig. 33. Velocity variation across the river at three selected transects for the flow rate of 4300 m<sup>3</sup>/s.

## Bed shear stress distribution for the flow rate of 4300 m<sup>3</sup>/s At three selected transects

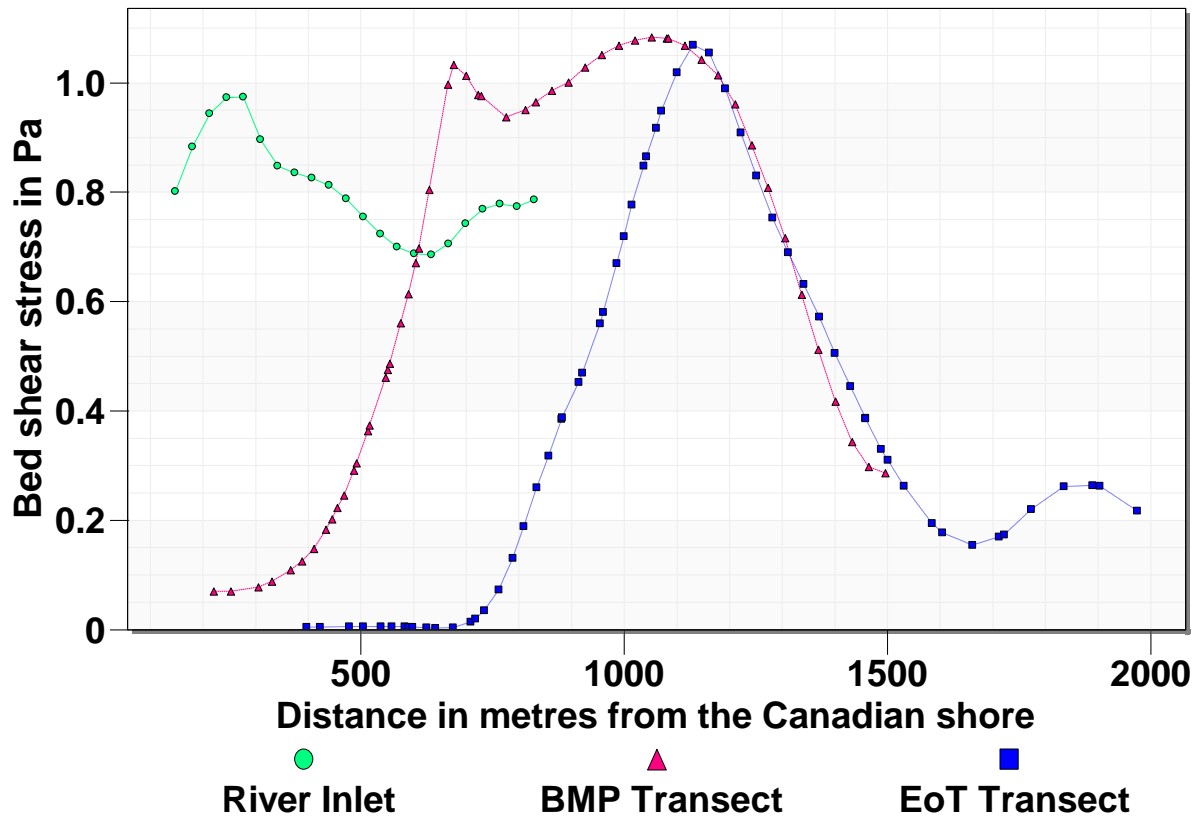


Fig. 34. Bed shear stress variation across the river at three selected transects for the flow rate of 4300 m<sup>3</sup>/s.

### Reassessment of sediment stability:

Using the simulations carried out for the three different flow conditions and using the sediment stability criteria developed in the earlier studies (see Krishnappan 2011), one can draw some conclusions regarding the stability of the deposited sediment in the BMP and EBMP areas. The sediment stability criteria reported in Krishnappan (2011) was based on in-situ erosion experiments carried out by Hans Biberhofer of ECCC in BMP and EBMP areas. These experiments showed that the sediment deposits in these areas are cohesive and were covered with an easily erodible fluff layer occupying a depth of about 5 cm. Under this fluff layer lies a consolidated cohesive bed with an erosion resistance of 0.29 Pa. To erode this consolidated deposit, the flow has to exert a bed shear stress greater than 0.29 Pa. This criterion will be tested using the refined grid model results for three discharges, namely, 2440 m<sup>3</sup>/s, 3657 m<sup>3</sup>/s and 4300 m<sup>3</sup>/s.

The bed shear stress distributions predicted by the model for the three discharges mentioned above are shown in Figs.35, 36 and 37.

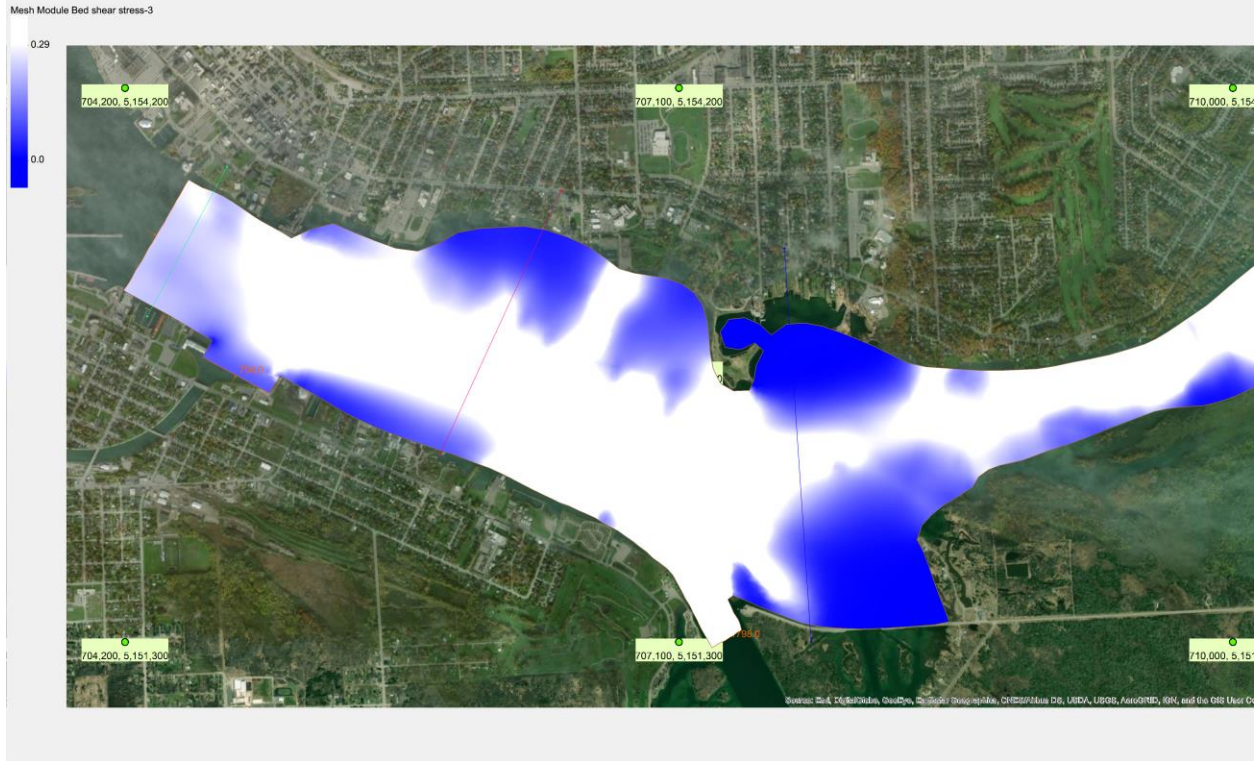


Fig. 35. Bed shear stress predicted by the refined grid model for the flow rate of 2440 m<sup>3</sup>/s.

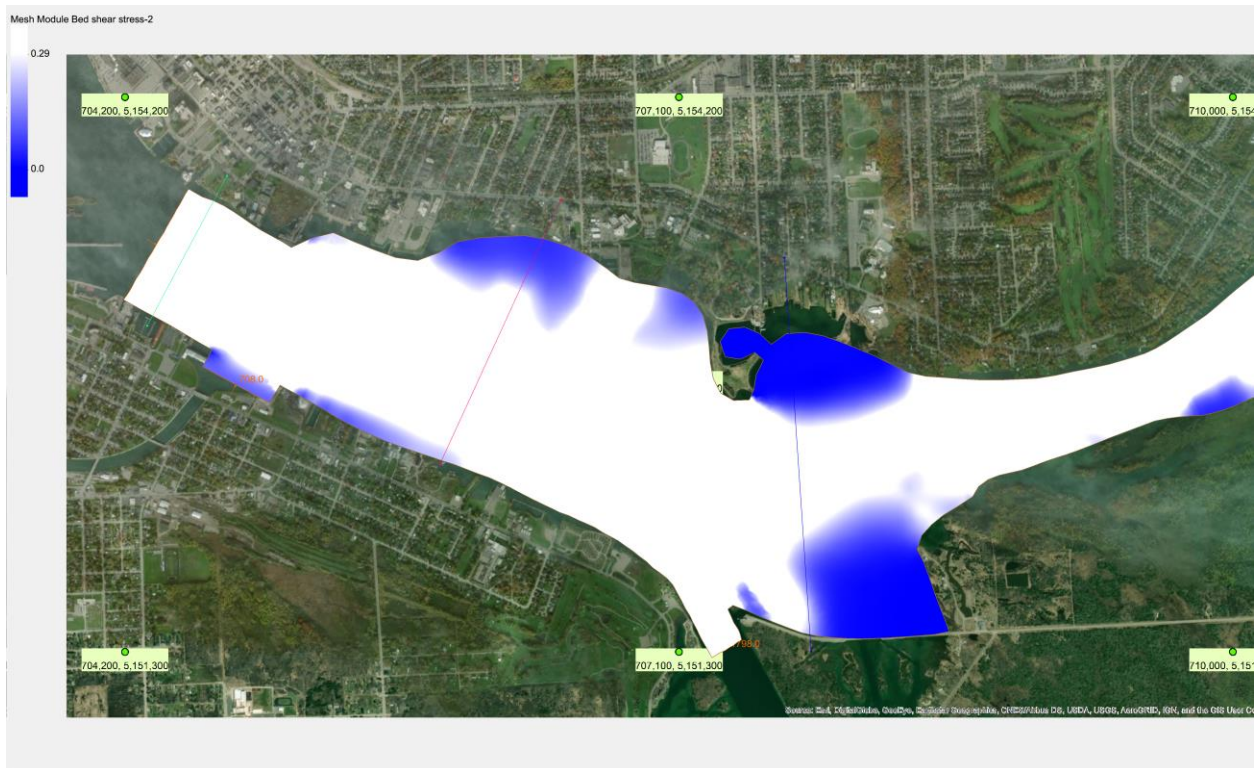


Fig. 36. Bed shear stress predicted by the refined grid model for the flow rate of 3657 m<sup>3</sup>/s.

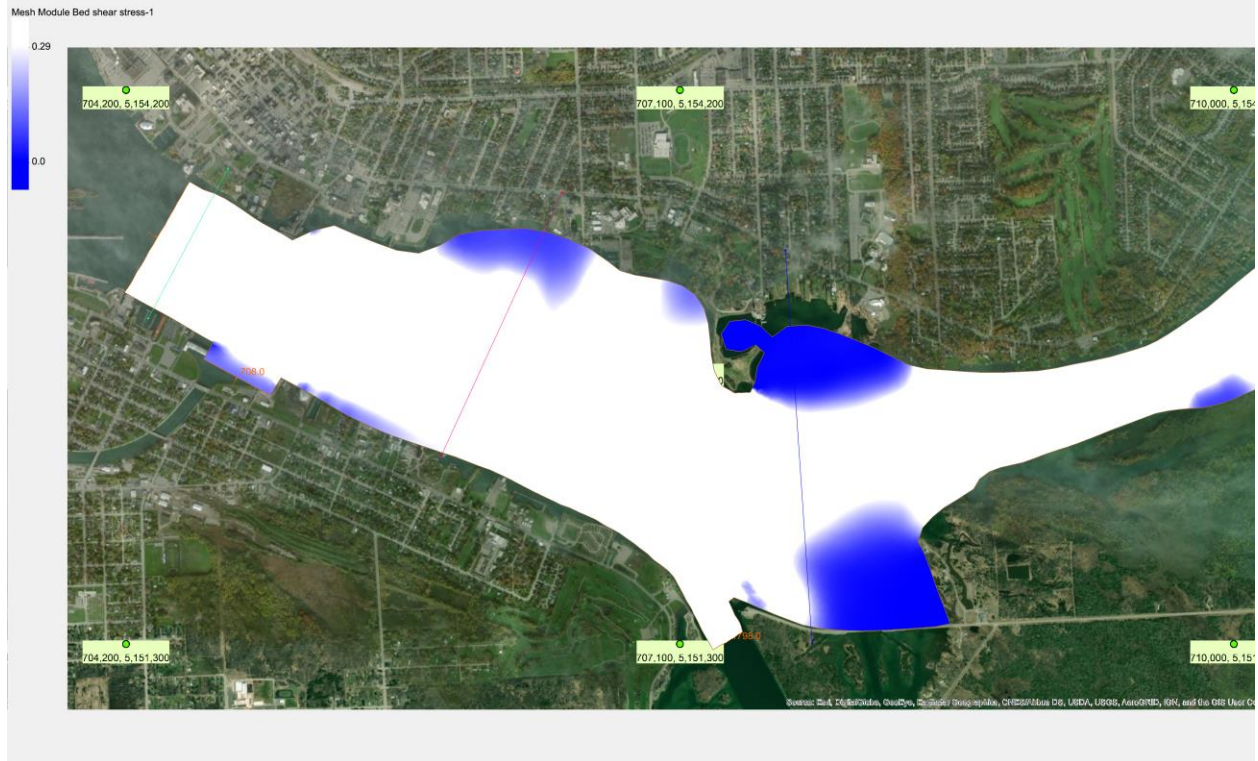


Fig. 37. Bed shear stress predicted by the refined grid model for the flow rate of 4300 m<sup>3</sup>/s.

In Figs. 35, 36 and 37, the areas of the region where the bed shear stress is below 0.29 Pa are shown in blue and the areas that have bed shear stresses above 0.29 Pa are shown in white. It can be seen from these figures that the blue region becomes smaller as the discharge increases as one would expect indicating that the areas with stable sediment deposits are becoming smaller and smaller. These figures also show that the BMP and EBMP areas have stable sediment deposits albeit becoming smaller as the flow rate increases.

To quantify the extent of the areas where sediment deposits are stable for the three different flow rates modelled, the variation of the bed shear stress along the transects BMP and EoT are examined as shown in Figs. 38 and 39. In Figs 38 and 39, the sediment stability criterion of 0.29 Pa is also included. From Fig. 38, it can be seen that as the flow rate increases the outer edge of the stable deposit area as given by the intersection of the 0.29 Pa line with the bed shear stress variation curve decreases as a function of the flow rate. For the BMP transect, these distances were estimated from Fig. 38 as 389 m for 2440 m<sup>3</sup>/s, 296 m for 3657 m<sup>3</sup>/s and 271 m for 4300 m<sup>3</sup>/s. For the EoT transects, the corresponding distances were estimated from Fig. 39 as 589 m for 2440 m<sup>3</sup>/s, 485 m for 3657 m<sup>3</sup>/s and 460 m for 4300 m<sup>3</sup>/s. These values are plotted in Fig. 40.

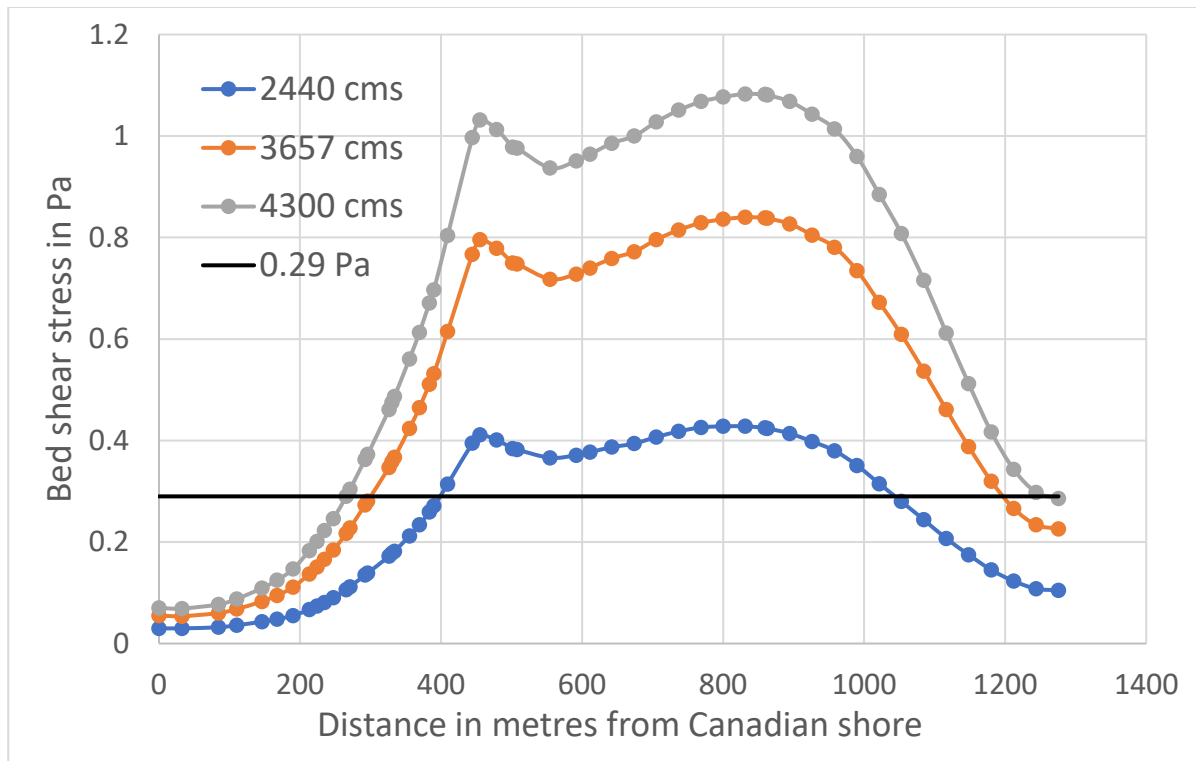


Fig. 38. Variation of bed shear stress along the BMP transect for the three flow rates modelled.

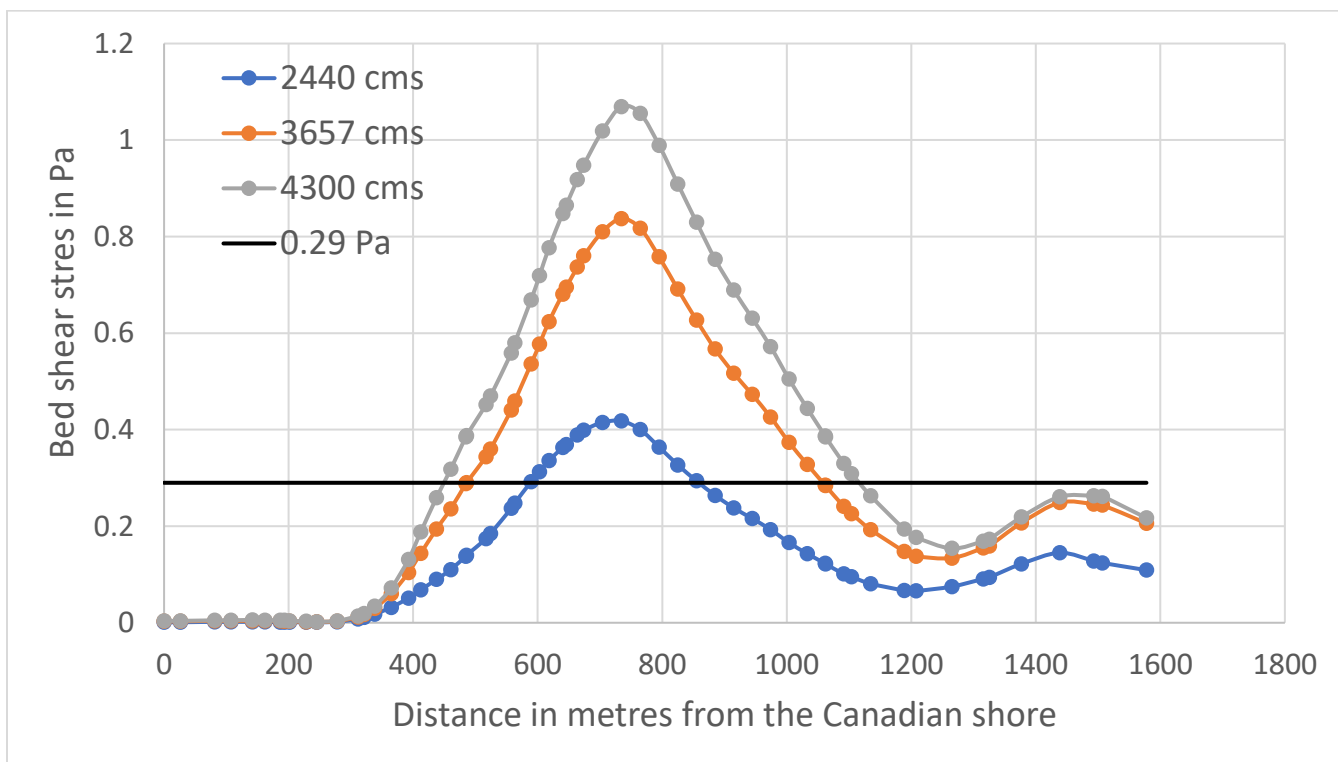


Fig. 39. . Variation of bed shear stress along the EoT transect for the three flow rates modelled.

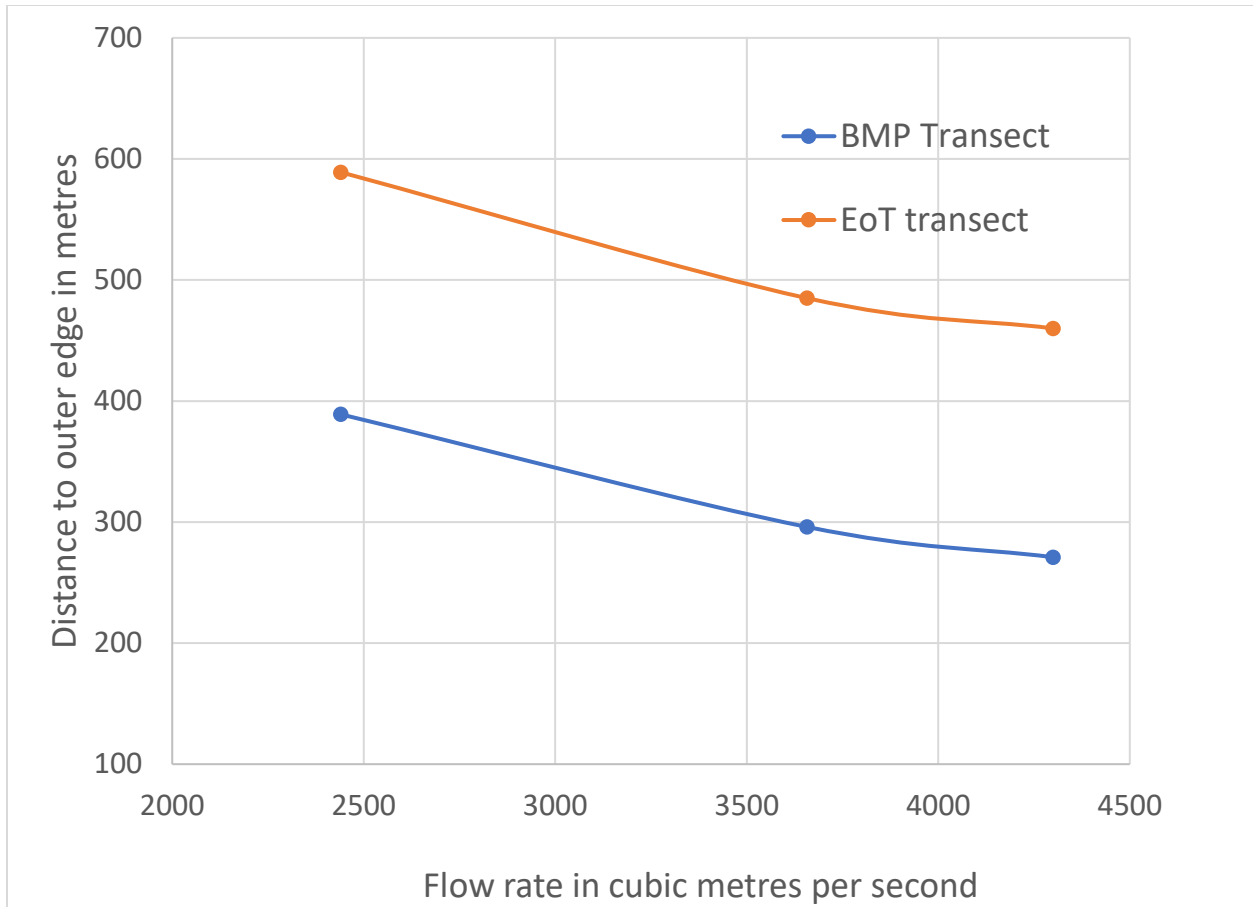


Fig. 40. Distance to outer edge of stable deposit as a function of flow rate modelled.

In Fig. 40 shows an interesting trend for the outer edge distance to to the flow rate in the river. As the flow rate increases the outer edge distance decreases and shows a levelling off trend. This means that with further increase in flow, the outer edge distance will not be affected as much implying that there will a stable deposition region in the BMP and EBMP areas permanently. This is a useful information for remediation strategy development for the area.

**Exportation of SMS solution files:**

Nodal values of flow characteristics such as velocity components, velocity magnitudes and bed shear stresses predicted by the refined grid model along with the positions of all 17989 nodes can be exported in ASCII file format for all the flow rates tested. This allows the stakeholders to use the flow data with their own measurement data in the field. The files will be made available to the technical authorities of the contract in the format of their choice.

## **Summary and conclusions:**

In this report, the sediment stability at Bellevue Marine Park (BMP) and area east of BMP (EBMP) in St. Mary's River near Sault Ste Marie was analysed using a modelling strategy developed by Krishnappan (2011). The original modelling work carried by Krishnappan (2011) used a coarse time scale of monthly average flows to analyse the stability of the sediment deposits in this area. In the current study, daily average flow rates measured during the time period from April 2002 to present were used together with a maximum flow rate that can be physically released from the lake were used to reassess the stability of the deeper contaminated sediment in BMP and EBMP areas. The numerical grid of the original model was also modified to refine the flow predictions in this area. The revised model was tested against original model to ascertain that the revised model was formulated correctly. A flow duration analysis of the flow data revealed that the flow regime in the river has shifted to a higher regime since 2014 and a 50% exceedance value for the new regime, which was calculated as 2440 m<sup>3</sup>/s was selected as one of the flows that will be tested with the refined grid model. The other flow rates that were selected for the model simulations were 3657 m<sup>3</sup>/s, which was highest recorded daily average flow rate measured on the 6<sup>th</sup> of August 2005, and 4300 m<sup>3</sup>/s, which was considered to be maximum flow that that can be physically released from the lake.

Model simulations were performed for these three flow rates and the flow properties including the bed shear stresses were calculated. Using the bed shear stress values and the sediment bed stability criterion developed by Krishnappan (2011), the stability of the sediment deposits in BMP and EBMP were reassessed. The reassessment confirmed that the extent of the stable sediment deposit area was a function of the flow rate and the area decreased as the flow rate increased. However, the decreament of the area showed a levelling off tendency, which suggests that a certain portion of the sediment deposits in this area are likely to be present for a foreseeable future.

## **Acknowledgements:**

The author wishes to thank Ms Kay Kim, the Senior Sediment Remediation Specialist, Great Lakes Area of Concern for giving me an opportunity to work on this study. A number of individuals from various government agencies and private companies had provided assistance to this study. The author wishes to thank them all. In particular, special thanks go to Aaron Thompson of Environment and Climate Change Canada for providing assistance with the RMA2 model. Jamie Ferguson of Environment and Climate Change Canada for provided flow data for the model. Mr. Scott Ellis of Cloverland Hydro electric Cooperative provided the flow data for the power plant. Hans Biberhofer of Environment and Climate Change Canada provided the background image for the refined grid model and guidance for the model study. The members of the study team provided helpful suggestions to carry out this study.

**References:**

B.G. Krishnappan 2011. Modelling of flow and sediment transport in the St. Mary's River near Sault Ste Marie. Report submitted to Environment Canada, Downsview, Ontario, Canada.

Aaron Thompson, Personal communication.

Hans Biberhofer, Personal communication.